SI MATERIALS AND METHODS

Statistical analyses.
For graphs and statistical analyses indicated we used GraphPad Prism 4.00, Statistica 8 (StatSoft) and SigmaPlot 10.0 software or R statistical environment. Normality of sampling distributions was tested with the Shapiro-Wilk W test (Statistica). For $W<0.05$ differences in means were tested for statistical significance with two-tailed Mann-Whitney test or Kruskal-Wallis test. For $W>0.05$ the Brown and Forsythe test was used for homoscedasticity (Statistica). For similar variances (Brown and Forsythe test, $P>0.05$) unpaired two-tailed Student's t-test was applied, for unequal variances (Brown and Forsythe test, $P<0.05$) unpaired two-tailed Welch's t-test was applied. *P*-values <0.05 were considered as statistically significant. Survival curves were compared with log-rank and Gehan-Wilcoxon tests.

Southern blot.
Genomic DNA was digested with BamHI. Hybridization was performed with a 337 bp probe labeled with ^{32}P-dATP or ^{32}P-dCTP, generated by PCR with the following primers: 5'-TGGGCACATGTGTTCATGCA-3' (sense) and 5'-CCCAGCTCTCTATGCCCTCA-3' (antisense). The BamHI digestion sites on the *tpl2* locus, the probe location and the size of the relevant DNA fragments are depicted in Fig. S3 *A* and *B*.

Total exudate peritoneal macrophages (TEPM).
TEPM were collected by peritoneal lavage from 10 week-old mice 3 days after a single i.p. injection of 1.0 ml 4% thioglycollate broth. TNF levels in culture supernatants were determined 6 hours upon stimulation with 1 μg/ml LPS from *Salmonella enteritidis* (SIGMA) by ELISA (eBioscience) according to the manufacturer's instructions.

Mice and design of in vivo experiments.
All mice were bred and maintained on a mixed C57BL/6J×129Sv genetic background in the animal facilities of the BSRC "Alexander Fleming" under specific pathogen-free conditions. *EIIaCre* transgenic (1), *ColVICre* transgenic (2) and *cox-2* conditional knock-out (3) mice have been previously described. *Tpl2*$^{-/-}$ mice (4) were kindly provided by Dr. P.N. Tsichlis, *LysMCre* transgenic mice (5) were kindly provided by Dr. I. Forster and *VillinCre* transgenic mice (6) were kindly provided by Dr. D.L. Gumucio. For all in vivo experiments 2-month old, littermate and sex-matched mice were used. Mice were randomly assigned to experimental groups on a first-come basis. No mice were excluded from analyses performed. All mice were used in accordance with the guidance of the Institutional Animal Care and Use Committee of BSRC "Alexander Fleming".

LPS/D-galactosamine-induced endotoxic shock.
Mice were injected i.p. with 10 μg LPS from *Salmonella enteritidis* (SIGMA) and 20 mg D-galactosamine dissolved in saline.

Induction of colitis.
Colitis was induced with 2.5% DSS (55 kDa; MP Biologicals) dissolved in the drinking water for the experimental days 1 to 7 followed by consumption of normal water for one more day. Experiments were performed with 2-month old, littermate, sex-matched and cohoused mice sharing identical conditions independent of their genotype. Mouse group size for DSS colitis experiments was calculated with Statistica software. To identify a 10% difference in body weight, with stardard deviation=8, alpha=0.05 (*P*-value) and beta=0.1 (90% power), sample size required was estimated to be n=15 mice. To establish differences observed reducing the probability for Type I errors, for alpha=0.001 and beta=0.1 sample size required was estimated n=30 mice.

Disease Activity Index calculation.
Disease Activity Index was calculated adding a) weight loss score (0-5% = 0; 5-10% = 1; 10-15% = 2; 15-20% = 3; >20% = 4), b) blood score (no blood visible = 0; blood traces in stool visible = 2; rectal bleeding = 4) and c) stool score (normal = 0; soft but formed = 2; very soft = 3; diarrhea = 4). For dead mice DAI = DAI max =12.

Histological assessment of DSS-induced colitis.
Tissues were fixed in formalin, embedded in paraffin and sections were stained with H&E or Periodic acid-Schiff reagent. Histopathological analysis was performed in the middle and terminal colon in a blind manner. Inflammation score was calculated adding a) inflammation severity score (mild = 1; moderate = 2; severe = 3), b) inflammation extent score (mucosal = 1; sub-mucosal = 2; transmural =3) and c) the mean of lymphoid follicles score (1-2 follicles = 1; 3-4 = 2; >4 = 3) and lymphoid aggregates score (1-3 aggregates = 1; 4-6 = 2; >7 = 3). Tissue damage score was calculated as the following sum [(normal area %) x 0 + (area with partial crypt loss %) x 1 + (area with extensive crypt loss %) x 2 + (area without crypts, epithelium still present %) x 3 + (ulcerated area %) x 4] /40 + depth of ulceration score (mucosal = 0; sub-mucosal = 1).

Isolation and FACS analysis of colonic lamina propria cells.
The colon was removed, flushed with HBSS/2%FBS, opened longitudinally and cut into 0.5 cm pieces. Tissue was then further washed and incubated in HBSS/2%FBS, 1 mM EDTA, 1mM DTT, at 37^{o}C in a shaking

waterbath for 45 min. The epithelial cells were released with vigorous shaking. Then, the tissue was washed and incubated in DMEM containing collagenase XI (50 units/ml, Sigma), dispase (0.1 mg/ml, Roche) and DNaseV (50 units/ml, Sigma) at 37^{o}C in a shaking waterbath for 2 hours. The resulting suspensions were layered on a discontinuous 67%/44% Percoll gradient (Sigma), centrifuged at 600 g for 20 min, and lamina propria lymphocytes were recovered from the interphase, washed and counted with a Coulter Counter. Single cell suspensions were stained for 30 min at 4^{o}C with antibodies against CD11b (FITC, eBioscience), Gr1 (Alexa647, Biolegend), TCRβ (eBioscience), CD4 (eBioscience) and CD8β (BD). For intracellular cytokine staining cells were incubated for 4 h with 50 ng/ml PMA (Sigma), 500 ng/ml Ionomycin (Sigma), and GolgiStop™ protein transport inhibitor containing monensin (BD). Intracellular staining was performed with mAbs against IL-10 (BD), IL-17 (eBioscience) and IFNγ (eBioscience). A FACSCanto II (BD Biosciences) flow cytometer was used for data acquisition. Analysis was performed with FACSDiva v.5.0 software.

FACS analysis of Cox-2 expression.
An FITC-conjugated Cox-2 antibody was used (Cayman 10010096, 1:250). Cells were fixed/permeabilized and intracellular staining was performed for 90 min with a buffer set purchased from eBioscience (00-5523-00). A FACSCanto II (BD Biosciences) flow cytometer was used for data acquisition. Analysis was performed with FACSDiva v.5.0 and WinMDI 2.9 software.

BrdU administration and staining.
Administration of BrdU (Sigma) was performed i.p. at a dose of 100 μg/g of body weight 2 hours prior to sacrification. BrdU immunostaining was performed in sections of paraffin embedded tissues using the BrdU In-Situ Detection Kit (BD Pharmingen) following manufacturer's instructions. The number of BrdU^{+} cells per crypt was measured by counting at least 20 well-oriented crypts per mouse in a blind manner.

Immunohistochemistry.
E-cadherin immunostaining was performed as described previously (7). Sox9 staining was performed in paraffin sections, upon antigen retrieval by boiling in citrate buffer for 30 min, with a rabbit polyclonal anti-Sox9 antibody (Santa Cruz, H-90) at a 1:100 dilution. α-SMA staining was performed in paraffin sections, upon antigen retrieval by boiling in citrate buffer for 30 min, with a FITC-conjugated monoclonal antibody (Sigma, 1A4) at a 1:500 dilution. A Nikon Eclipse E800 microscope was used and photos were taken through a Nikon Dxm1200F camera and ACT1.1 software.

Isolation of mouse colonic myofibroblasts.
Colonic myofibroblast isolation was performed as described elsewhere (8). Briefly, colons from 7-9 days-old pups were dissected, washed with HBSS containing antibiotics, cut in 2-3 mm pieces and incubated with 300 U/ml Collagenase XI (Sigma) and 0.1 mg/ml Dispase (Roche) in DMEM for 90 min at 25°C. After low speed centrifugation the pellet was minced, further washed with 2% sorbitol, centrifuged at 200 g for 5 min and plated in a 6-well plate in DMEM containing 1% L-Glutamine (Gibco), 1% non-essential amino acids (Gibco), 1% penicillin-streptomycin (Gibco) and 10 ng/ml Gentamicin (Gibco). At passage 6, cells were checked for purity using FACS analysis. To exclude the presence of contaminating cells, IMF cultures were tested by FACS analysis as previously described (9). Cells that were >80% positive for CD90.2 (Biolegend) and <2% for CD45 (BD Biosciences) were used for subsequent experiments till passage 9. Cells were stimulated with 10 ng/ml IL-1β (Peprotech) or 10 μg/ml LPS from *Salmonella enteritidis* (SIGMA).

TNBS colitis.
TNBS colitis was performed in littermate, sex-matched and cohoused mice sharing identical conditions independent of their genotype, on a mixed C57BL/6J×129Sv genetic background. On day -7 mice were anaesthetized, shaved on the top of the back area and a presensitization solution was applied (1% TNBS dissolved in acetone:olive oil 4:1 v/v). On day 0, mice were anaesthetized and induction solution was intrarectally instilled (4% TNBS in 40% ethanol). TNBS was purchased from Sigma. Colons were harvested on day 3 post-induction. Histopathological analysis was performed in H/E-stained sections in the middle and terminal colon in a blind manner. Inflammation score was calculated adding a) inflammation severity score (mild = 1; moderate = 2; severe = 3), b) inflammation extent score (mucosal = 1; sub-mucosal = 2; transmural = 3) and c) % area involved score (1-25 % = 1; 26-50 % = 2; 51-75 % = 3; 76-100 % = 4). Tissue damage score was calculated as the following sum [(normal area) x 0 + (area with partial crypt loss) x 0.2 + (area with extensive crypt loss) x 0.3 + (area without crypts, epithelium still present) x 0.5 + (area with mucosal ulceration) x 0.7 + (area with sub-mucosal ulceration) x 0.8 + (area with transmural ulceration and necrosis) x 1. The extent of each area was estimated as following: focal observation = 0.5; extending in half a field = 1; in 1 field = 2; in 2 fields = 4; in 25% of the tissue = 5; in >50% of the tissue = 10.

Sample preparation and Mass Spectrometry analysis for prostanoids
Prostanoids were extracted with acetone followed by liquid/liquid extraction as previously described (10), with some modifications. Briefly, 70 μl supernatant samples from IMFs cultured in 48-well plates were deproteinized with acetone. After vortexing for 4 min and centrifugation at 2000 g for 10 min at 4^{o}C, samples were transferred to a clean 15 ml glass vial, mixed with 800 μl of hexane by vortexing for 0.5 min and centrifuged for 10 min at 2000 g at 4^{o}C. The lower phase was acidified to pH 3.5 with formic acid and then mixed with chloroform. After

vortexing for 0.5 min and centrifugation for 10 min at 2000 g at 4°C, the lower chloroform phase was kept for 15 min at -80°C to separate any residual from the upper phase. Samples extracted in chloroform were evaporated to dryness using a speed-vac concentrator (Savant, model #SC110-120) and redissolved in 100 μl of methanol/100 mM ammonium acetate pH 8.5 (9:1). 16,16-dimethylo PGE_2 (Cayman) was used as an internal control in each sample from the beginning of the above extraction procedure at a final concentration of 2.5 ng/ml. Samples were analysed by direct infusion in a LTQ Orbitrap XL mass spectrometer (Thermo Scientific, Waltham, MA, USA) with electrospray ionization in negative mode. Capillary temperature was 275°C, Spray Voltage was 3.5 kV, Sheath Gas was set at 40 units and Sweep Gas at 8 units. The resolution was 100 K providing high accuracy for prostanoid measurements. Precursor ion masses were used for prostanoid profiling while lipid identity was confirmed by precursor ion fragmentation using collision induced dissociation (CID). Precursor m/z 297.1530 was used for 13,14-dihydro-15-keto-tetranor-PGE_2 and tetranor-PGE_1, stable metabolites of PGE_2. Precursor m/z 353.2030 was used for metabolites downstream of PGH_1 and PGH_2 including PGD_1, PGE_1, 13,14-dihydro-15-keto-PGE_1, $PGF_{2\alpha}$, 8-iso-$PGF_{2\alpha}$, 11-β-13,14-dihydro-15-keto-$PGF_{2\alpha}$, and 11-β-$PGF_{2\alpha}$.

In vivo dmPGE_2 administration.
16,16-dimethyl prostaglandin E_2 (dmPGE_2) dissolved in methyl acetate was purchased from Cayman. After methyl acetate was evaporated under a nitrogen stream, dmPGE_2 was immediately dissolved in nitrogen-purged ethanol and kept as a stock solution at a concentration of 0.5 mg/ml. For in-vivo experiments, the stock dmPGE_2 solution was diluted with saline immediately before use and kept on ice. dmPGE_2 solution was administered i.p. at a dose of 10 μg/kg of body weight twice daily (every 12 hours) concurrently with DSS treatment. Control mice received a similar volume of saline. To detect an effect of dmPGE_2 in rescuing the difference in body weight between *Tpl2*$^{D/D}$ mice and WT controls (11% of initial body weight, standard deviation=8), with alpha=0.05 and beta=0.2, the sample size required was calculated with Statistica software to be n=10 mice.

TNF-induced epithelial cell death and TUNEL assays.
Mice were injected i.v. with 12 μg mouse recombinant TNF (kindly provided by Dr. Claude Libert, Ghent University, Belgium) and sacrificed 1 hour later. The extent of TNF-induced epithelial cell death was assessed by TUNEL assays performed in paraffin sections of the terminal ileum. TUNEL assays in DSS-treated or TNF-treated mice were performed in paraffin sections of the colon or ileum respectively with the DeadEnd™ Fluorimetric TUNEL System (Promega) or the TACS® 2 TdT-DAB *In Situ* Apoptosis Detection Kit (Trevigen) according to the manufacturer's instructions.

Western blot.
We used antibodies against Tpl2 (rabbit polyclonal, M20, Santa Cruz), Sox9 (rabbit polyclonal, H90, Santa Cruz), Cox-2 (rabbit polyclonal, Cayman), p-ERK (mouse monoclonal, Santa Cruz), ERK2 (rabbit polyclonal, Santa Cruz), p-JNK (mouse monoclonal, Cell Signaling), JNK (mouse monoclonal, Santa Cruz), p-CREB (Ser133) (rabbit monoclonal, Cell Signaling), CREB (rabbit monoclonal, Cell Signaling), IκB-α (rabbit polyclonal, C21, Santa Cruz) and β-actin (goat polyclonal, Santa Cruz).

RT-PCR analysis.
RNA extraction from mouse tissues and primary cells was performed using TRIZOL reagent (Invitrogen) according to manufacturer's instructions. 12 μg of total RNA was treated with RQ1 DNase I (Promega), purified by SDS-containing phenol/chloroform and ethanol precipitation and used to generate cDNA templates using M-MLV RT (Promega) and oligo-dT primers. To detect the normal *tpl2* (*map3k8)* transcript and validate the efficient excision of exon 4 in knock-out mice we used a sense primer in exon 3 (5'-TTAGCCCAAGACATGAAGAC-3') and an antisense primer in exon 4 (5'-ACTCAGCAATGTTCTCATGC-3'). Quantitative RT-PCR was performed with a Chromo4 Real-Time PCR detection system (Bio-Rad Laboratories) using Platinum SYBR Green (Invitrogen). All data were normalized to β2-microglobulin (β2m) expression. The following oligonucleotides were used for murine genes: B2Mf (5'-TTCTGGTGCTTGTCTCACTGA-3'), B2Mr (5'-CAGTATGTTCGGCTTCCCATTC-3'), TNFf (5'-CACGCTCTTCTGTCTACTGA-3'), TNFr (5'-ATCTGAGTGTGAGGGTCTGG-3'), IL-18f (5'-CAGGCCTGACATCTTCTGCAA-3'), IL-18r (5'-TCTGACATGGCAGCCATTGT-3'), ccl2f (5'-AGCACCAGCACCAGCCAACT-3'), ccl2r (5'-TTCCTTCTTGGGGTCAGCAC-3'), ccl5f (5'- GCCCTCACCATCATCCTCAC-3'), ccl5r (5'-CTTCTCTGGGTTGGCACACA-3'), ptgs2f (5'-TCAGTTTTTCAAGACAGATC-3'), ptgs2r (5'-TCTCTACCTGAGTGTCTTTG-3') and Qiagen's QuantiTect primers for ptgs1 (QT00155330). Data were analyzed with RelQuant software (Bio-Rad Laboratories).
RNA from human primary IMFs was extracted using the RNeasy Mini Kit (Qiagen) according to the manufacturer's instructions. Reverse transcription was performed using QuantiTect Reverse Transcription Kit (Qiagen) and Q-PCR for *B2M*, *MAP3K8* and *PTGS2* with QuantiTect Primer Assays (Qiagen: QT00013454, QT00051730, QT00040586).

Methylene blue staining of colon whole mounts.
Tissues were fixed in formalin, stored overnight in 70% ethanol, stained with PBS containing 0.3% methylene blue (Sigma) for 40 min and observed within next hours using a Nikon TE300 microscope.

Myeloperoxidase (MPO) activity in the colon.
Tissue samples were homogenized in 50 mM potassium phosphate (pH 6) containing 0.5% hexadecyltrimethylammonium bromide (Sigma) and 5 mM EDTA and centrifuged at 2,000 rpm. The homogenate was freezed/thawed three times, centrifuged at 15,000 rpm, 4 ^{o}C for 15 min and the protein concentration was measured with a Bradford assay. For the measurement of enzymatic activity in 50 μl homogenate were added 100 μl 50 mM potassium phosphate (pH 6) containing 0.25 mg/ml o-dianisidine and 0.05% H_2O_2. The change of absorbance at 460 nm was measured for 10 min. The results were expressed as ΔOD /min /mg of protein. Addition of the MPO inhibitor NaN_3 at a final concentration 0.1% was used to test the specificity of the assay.

Isolation of intestinal epithelial cells and colonic stromal cells.
The colon was removed, flushed with HBSS/2%FBS, opened longitudinally and cut into 0.5 cm pieces. The tissue was further washed and incubated in HBSS/2%FBS, 0.5 mM EDTA, 1 mM DTT, at 37^{o}C in a shaking waterbath for 45 min. Upon vigorous shaking the cell suspension released was layered on a discontinuous 25%/40% Percoll gradient (Sigma) and centrifuged at 600 g for 10 min. IECs were collected from the interphase. The purity of the population was assessed by FACS analysis for the epithelial marker E-cadherin (FITC-conjugated mAb, BD) and was consistently ~90%. The isolation of colonic stromal cells was performed upon an additional 30 min incubation in 1 mM EDTA, 1 mM DTT followed by vigorous shaking for the complete depletion of IECs. Then, the tissue was incubated in HBSS/2%FBS containing 500 U/ml Collagenase XI (Sigma) and 0.1 mg/ml Dispase (Roche) for 90 min and the cells collected were washed and cultured in DMEM supplemented with 10% FBS, 100 U/ml penicillin, and 100 μg/ml streptomycin (Invitrogen). After 24 hours of culture the cells attached to the dishes were collected for protein extraction.

Expression profiling of colonic myofibroblasts with next-generation sequencing.
Primary colonic myofibroblasts were isolated from *Tpl2*$^{D/D}$ and WT control mice and cultured as described above in 2 independent experiments. In each experiment RNA was isolated from cells 1) remained untreated, 2) stimulated with 10 ng/ml IL-1β (Peprotech) for 24 hours, 3) stimulated with 10 μg/ml LPS from *Salmonella enteritidis* (SIGMA) for 24 hours. In 2 additional independent experiments RNA was isolated from primary colonic myofibroblasts from *Tpl2*$^{D/D}$ and WT control mice which remained untreated. Total RNA was extracted with TRIZOL reagent (Invitrogen). Polyadenylated RNA (polyA-RNA) was isolated from 6 μg of total RNA using the Dynabeads Oligo(dT) kit (Ambion, Life Technologies Corporation). The purified polyA-RNA preparation was randomly fragmented by chemical hydrolysis at 94^{o}C for 5 minutes. The fragmented polyA-RNA was treated with antarctic phosphatase to remove phosphate groups from the fragments' ends, followed by treatment with T4 polynucleotide kinase to add a Pi at the 5' end of each fragment. The resulting RNA fragments were hybridized and ligated to the P1 and P2 adaptor sequences specifically designed for sequencing with the SOLiD system (SOLiD Total RNA-Seq Kit, Life Technologies Corporation). The RNA produced was reverse transcribed to cDNA which was then amplified in a 15-cycle PCR. At this step, the use of different barcoded 3' PCR primers from the selection included in the SOLiD barcoding kit allowed the preparation of cDNA libraries for multiplex sequencing. From the cDNA produced, only fragments of average size 200-300 bp were selected with two rounds of magnetic bead purification (Agencourt AMPure XP Reagent, Beckman Coulter). The quality and size of the purified cDNA library was assessed on the Agilent Bioanalyzer 2100 (Agilent Technologies Inc.) and with quantitative PCR using the Library Quant Kit ABI Solid (KAPA Biosystems). A multiplex library mix (500 pM) was used to prepare a full-slide for analysis on the SOliD 4 Sequencing System (Applied Biosystems) with 35+50 bp PE –chemistry.

Detection of differentially expressed genes, Gene Set Enrichment Analysis, construction of functional interaction networks and transcription factor inference.
The TopHat v2.0.5 software (11) was used to map reads to the reference genome (mm9) and the Cufflinks 2.02 package (12) to estimate the level of gene expression represented by value of fragments per kilobase of exon model per million (FPKM) and differential expression for all genes as annotated by Ensembl. For the untreated samples, genes were sorted with descending average fold-change values compared to WT controls. 423 consistently deregulated genes were selected on the basis of a) reproducible fold-change direction in all four experimental replicates, b) significant (p-value <0.05, q-value <0.01) fold-change in at least one out of four experimental samples. Top and bottom 20 genes were presented as heatmaps. Functional interrogation of deregulated genes was performed through gene set enrichment analyses at the level of Gene Ontology and KEGG Pathways with the use of a custom Perl script designed to exhaustively assess the enrichment for each gene set under question. For the IL-1β and LPS treated samples, genes were classified according to fold-change values compared to untreated controls. 110 and 144 genes were respectively selected on the basis of being a) consistently deregulated (same direction) in two experimental replicates and b) significantly deregulated (p-value <0.05, q-value <0.01) in both samples. Average fold-change values from the two experimental replicates were clustered with average linkage hierarchical clustering and clusters were represented as heatmaps with the use of the R statistical environment. Functional interaction networks of genes induced in WT colonic myofibroblasts by IL-1β or LPS (95 and 121 genes respectively) were generated with STRING v9.0 database software (13) and visualized with Cytoscape v2.8.3 software (14, 15). Genes showing a Tpl2$^{D/D}$ minus WT expression fold change difference <-0.8 were considered as defectively induced in Tpl2$^{D/D}$ cells. Transcription factor inference from differentially expressed genes was performed by using

Enrichr (TRANSFAC and JASPAR PWMs) (16) and WebGestalt (17) software. Only murine transcription factors predicted by both applications (adjusted p-value <0.05) were considered.

Patients.
Intestinal tissues were obtained from surgical specimens taken from patients suffering from Crohn's disease or ulcerative colitis. Healthy areas of intestine taken from patients admitted for bowel resection because of colon cancer or diverticulosis were used as controls. The clinical data of IBD patients are summarized in Table S4. Specimens were frozen in Cryoblock Compound (DiaPath) on dry ice and stored at -80°C. Human studies were approved by the Ethical Committee of Istituto Clinico Humanitas.

Primary human intestinal myofibroblasts (hIMFs).
hIMFs were isolated from inflamed and un-inflamed area of IBD and from controls as follows: Briefly, after rapid rinsing with cold HBSS without calcium and magnesium (HBSS-/-), the intestinal mucosa was removed from the specimens. 5-10 strips of mucosa (each 3 x 1 cm) were placed into 2 mM DTT (Sigma) solution for 15 min at room temperature spinning at low speed on magnetic stirring bar. After this time, the strips were incubated in 1mM EDTA solution for 1 hour at 37°C under constant slow agitation. After extensive washing, the tissues were digested for 1 hour in RPMI medium supplemented with 5% FCS, 10 mM HEPES, 0.75 mg/mL collagenase type II, and 20 µg/mL DNase I (both from Worthington Biochemical Corporation, Lakewood, NJ). The cell-pellet was resuspended in DMEM without L-glutamine medium (Gibco) supplemented with 10% FCS (Gibco), 1 M HEPES, 200 mM L-Glutamin (Lonza), and Penicillin / Streptomycin and the cells were cultured in uncoated plates at 50000 cells per cm^2. After 1 day, non-adherent cells were removed and fresh Medium 106 (Invitrogen Cat. No. M-106-500) supplemented with 10 ml of low serum growth supplement (LSGS, Invitrogen Cat. No. S-003-10) was replaced. Once the cells reached confluence, they were detached using trypsin/EDTA for 5 min at 37°C and sorted negatively for CD31-FITC (BD pharmigen n° 555445) and CD45-PerCP (human Immunological Sciences n° MAB-142CP) surface markers by flow cytometry. The sorted cells were kept in culture and expanded using Medium 106 supplemented with 10 ml of low serum growth supplement and characterized for the expression of α-SMA, vimentin and desmin markers by immunofluorescence analysis. The cells were tested between passage 4 to 6.

eQTL analysis.
Cis-eQTL analysis was performed in all data available through the Genevar database (Sanger Institute) in a region ±100 kb around *MAP3K8* transcription start site. Only SNPs and indels included in the ~115 kb *MAP3K8* gene region surrounded by the two recombination hotspots shown in Fig. S1*A* were considered. Significance was evaluated by 10,000 permutations by Genevar software. Human Epigenome's Project colonic mucosa data were accessed through NIH Roadmap Epigenomics Project Data Listings.

Table S1

Physical or functional interactions between Tpl2 and other IBD-associated genes based on the literature.

IBD-associated gene in GWAS	Interaction with Tpl2	Cell type
NFKB1 (p105)	Physical interaction (18, 19)	
RELA	Physical interaction (19)	
CD40	Upstream activator of Tpl2 signaling	B cells (20)
NOD2	Upstream activator of Tpl2 signaling	Macrophages (21)
IL1R1	Upstream activator of Tpl2 signaling	Fibroblasts (22)
MAPK1 (ERK2)	Mediator of Tpl2 signaling	Macrophages (4), Fibroblasts (22), B cells (20), T cells (23), Dendritic cells (24), Kupffer cells (25), Hepatic Stellate cells (25), Mast cells (26)
STAT3	Mediator of Tpl2 signaling	Macrophages (27)
STAT4	Mediator of Tpl2 signaling	T cells (28)
FOS (c-Fos)	Downstream target	Macrophages (24), cell lines (29)
ATF4	Downstream target	Osteoblasts (30)
NOS2	Downstream target	Macrophages (31)
CCL2	Downstream target	Macrophages (32)
CXCL2	Downstream target	Macrophages (32)
CXCL3	Downstream target	Macrophages (32)
IL8	Downstream target	Fibroblast-like synoviocytes (33)
IL2	Downstream target	T cells (34)
IL4	Downstream target	T cells (35)
IL5	Downstream target	T cells (35), Mast cells (26)
IL13	Downstream target	Mast cells (26)
IL12B (p40)	Downstream target	Macrophages (21, 36), Dendritic cells (36)
IL10	Downstream target	Mast cells (26), Kupffer cells (25), Macrophages (24), Dendritic cells (24)
IFNG	Downstream target	T cells (28)
IFNAR, *IFNAR2*	Receptor of the downstream target type I interferon	Macrophages, Dendritic cells (24, 37)
IL23R	Receptor of the downstream target IL-23p19	Macrophages (30), Kupffer cells (25)
PTGER4	Receptor of the downstream target prostaglandin E_2	Macrophages (38), T cells (39)

Table S2

Gene Ontology pathways containing at least 50 genes each consistently enriched among genes which are differentially regulated upon treatment in Tpl2 deficient intestinal myofibroblasts as compared to WT controls in two independent experiments.

IL-1β	
extracellular space	2.31553
inflammatory response	2.17548
proteinaceous extracellular matrix	2.12266
extracellular matrix	2.09620
wound healing	2.06078
heparin binding	1.88372
basement membrane	1.80671
extracellular region	1.74196
response to lipopolysaccharide	1.70872
iron ion binding	1.68815
cell adhesion	1.56353
LPS	
serine-type endopeptidase inhibitor activity	2.68395
immune response	2.68053
extracellular space	2.25287
chemotaxis	2.24341
basement membrane	2.17741
proteinaceous extracellular matrix	2.05837
response to lipopolysaccharide	1.85251
external side of plasma membrane	1.83696
response to stimulus	1.79414
extracellular region	1.76364
extracellular matrix organization	1.75721
growth factor activity	1.74288
G-protein coupled receptor protein signaling pathway	1.70491
G-protein coupled receptor activity	1.50132

Table S3

Rare variants in human *MAP3K8* gene (Minor Allele Frequency <0.01) predicted to exert a deleterious effect on protein function.

Variant ID	Chr: bp	Alleles	Class	Type	Amino acid		SIFT	PolyPhen	Protein domain
rs201540136	10:30736750	G/A	SNP	Missense variant	126	Asp/Asn	0.011	0.995	
rs201892819	10:30736792	G/T	SNP	Missense variant	140	Gly/Cys	0.001	1.001	Catalytic domain
TMP_ESP_10_30736810	10:30736810	C/T	SNP	Missense variant	146	Arg/Trp	0.011	0.984	Catalytic domain, ATP binding
rs3087944	10:30739323	C/T	SNP	Missense variant	214	Ser/Phe	0.001	0.990	Catalytic domain
TMP_ESP_10_30747010	10:30747010	C/T	SNP	Splice region variant	-	-	-	-	Catalytic domain
rs66989210	10:3074703010:30747030	G/-	deletion	Frameshift variant	297		-	-	Catalytic domain
rs78570736	10:30748177	T/G	SNP	Splice region variant	-	-	-	-	
rs138733925	10:30748326	C/T	SNP	Missense variant	390	Pro/Leu	0.031	0.976	
TMP_ESP_10_30748438	10:30748438	C/T	SNP	Splice region variant	-	-	-	-	
rs145710720	10:30749658	G/A	SNP	Missense variant	433	Glu/Lys	0.011	0.979	
rs139316352	10:30749700	G/A	SNP	Missense variant	447	Asp/Asn	0.041	0.854	
TMP_ESP_10_30749719	10:30749719	G/C	SNP	Missense variant	453	Gly/Ala	0.001	0.994	

MAP3K8 (TPL2, COT) protein: 467aa, protein kinase-like domain: aa 120-448
Minor Allele Frequency of all variants <0.01
Variant sources: dbSNP, NHLBI Exome Sequencing Project
Prediction of variation effect on protein function (ENSEMBL): SIFT tool (<0.05 deleterious), PolyPhen tool (>0.900 probably damaging)
Prediction of MAP3K8 domains: PROSITE

Table S4

Clinical characteristics of IBD patients and control subjects.

	Crohn's Disease n=9	**Ulcerative Colitis n=8**	**Control n=5**
Age (Years)	46.50 ± 14.30	53.25 ± 13.50	48.12 ± 9.93
Gender (Men/Women)	5 / 4	4 / 4	4 / 1
Site of lesion			
Ileum	6	1	-
Colon	3	7	5
Duration of IBD (Years)	14.10 ± 8.20	13.30 ± 5.80	-
Medications			
Mesalazine	-	3	
Antibiotics	1	-	
Steroids	-	-	
Immunomodulators	1	2	
Biologics	2	-	
None	5	3	
Resistance to drugs	9	8	
Resistance to aminosalicylates	4	3	

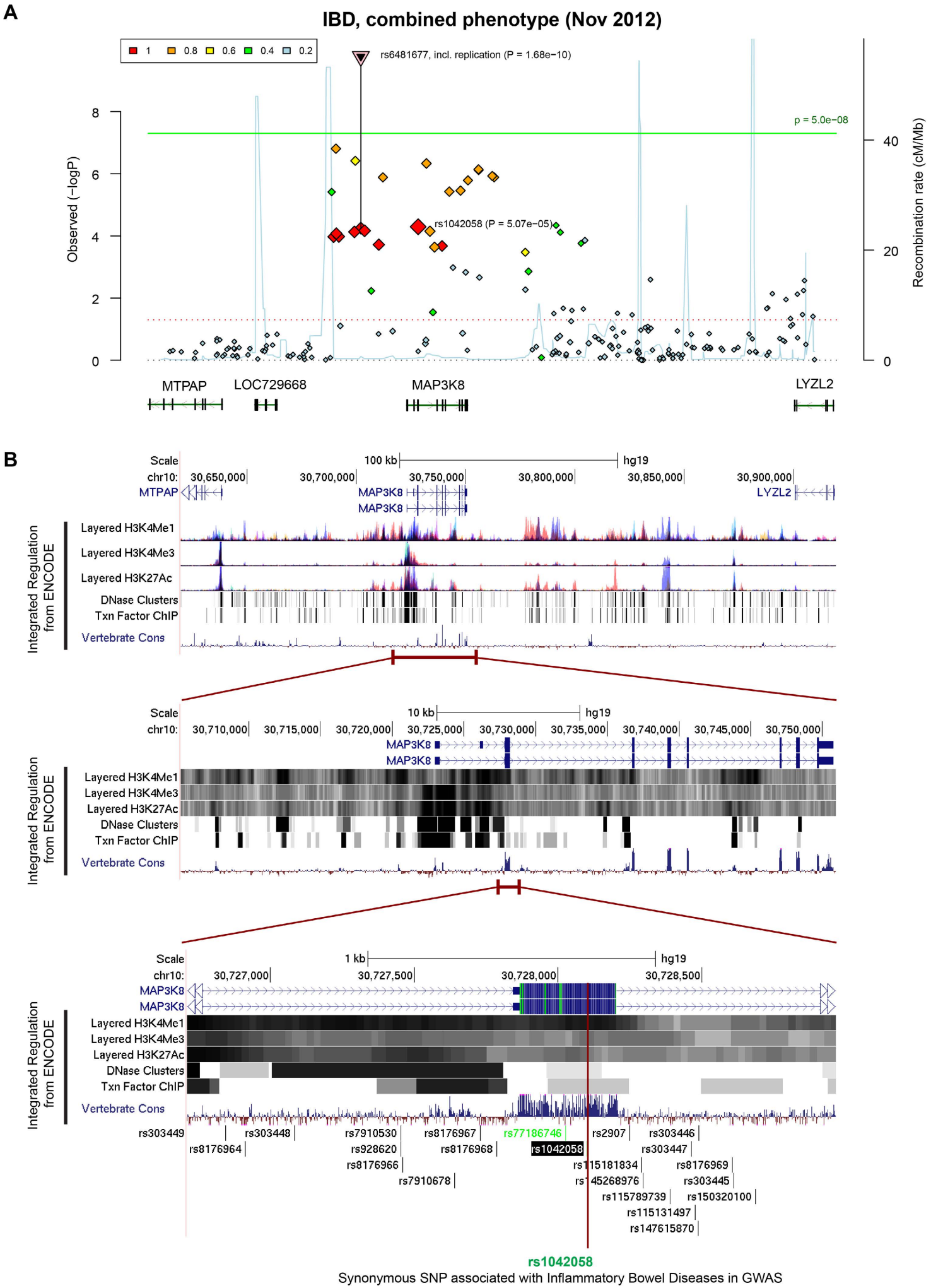
A
IBD, combined phenotype (Nov 2012)
1
0.8
0.6
0.4
0.2
rs6481677, incl. replication (P = 1.68e−10)
p = 5.0e−08
rs1042058 (P = 5.07e−05)
Observed (−logP)
Recombination rate (cM/Mb)
MTPAP
LOC729668
MAP3K8
LYZL2
B
Scale
100 kb
hg19
chr10:
30,650,000
30,700,000
30,750,000
30,800,000
30,850,000
30,900,000
MTPAP
MAP3K8
MAP3K8
LYZL2
Integrated Regulation from ENCODE
Layered H3K4Me1
Layered H3K4Me3
Layered H3K27Ac
DNase Clusters
Txn Factor ChIP
Vertebrate Cons
10 kb
30,710,000
30,715,000
30,720,000
30,725,000
30,730,000
30,735,000
30,740,000
30,745,000
30,750,000
1 kb
30,727,000
30,727,500
30,728,000
30,728,500
rs303449
rs303448
rs7910530
rs8176967
rs77186746
rs2907
rs303446
rs8176964
rs928620
rs8176968
rs1042058
rs303447
rs8176966
rs115181834
rs8176969
rs7910678
rs145268976
rs303445
rs115789739
rs150320100
rs115131497
rs147615870
rs1042058
Synonymous SNP associated with Inflammatory Bowel Diseases in GWAS

Figure S1

SNP rs1042058 associated with IBD in GWAS is located in exon 2 of *MAP3K8* gene.

(*A*) IBD association plot of the *MAP3K8* gene region showing strength of association (-log10 *P*-value) and recombination rates (cMorgan/Mb). SNPs are colored based on linkage disequilibrium with rs1042058 which has been validated to be associated with IBD (40). Data visualization was performed with Ricopili software based on the November 2012 combined IBD phenotype GWAS dataset (40).

(*B*) UCSC genome browser display showing ENCODE's Integrated Regulation data(41) for the human *MAP3K8* gene region shown in (*A*). The synonymous SNP rs1042058 associated with IBD pathogenesis in GWAS (40) is located in exon 2 in a region containing active regulatory elements. H3K4Me3 mark is associated with promoters and transcription starts, H3K4Me1 is a mark of regulatory elements associated with enhancers and other distal elements but also enriched downstream transcription starts, H3K27Ac is a mark of active regulatory elements, DNaseI hypersensitivity indicates chromatin accessibility and is the hallmark of regulatory regions and ChIP-seq data show transcription factor binding (41).

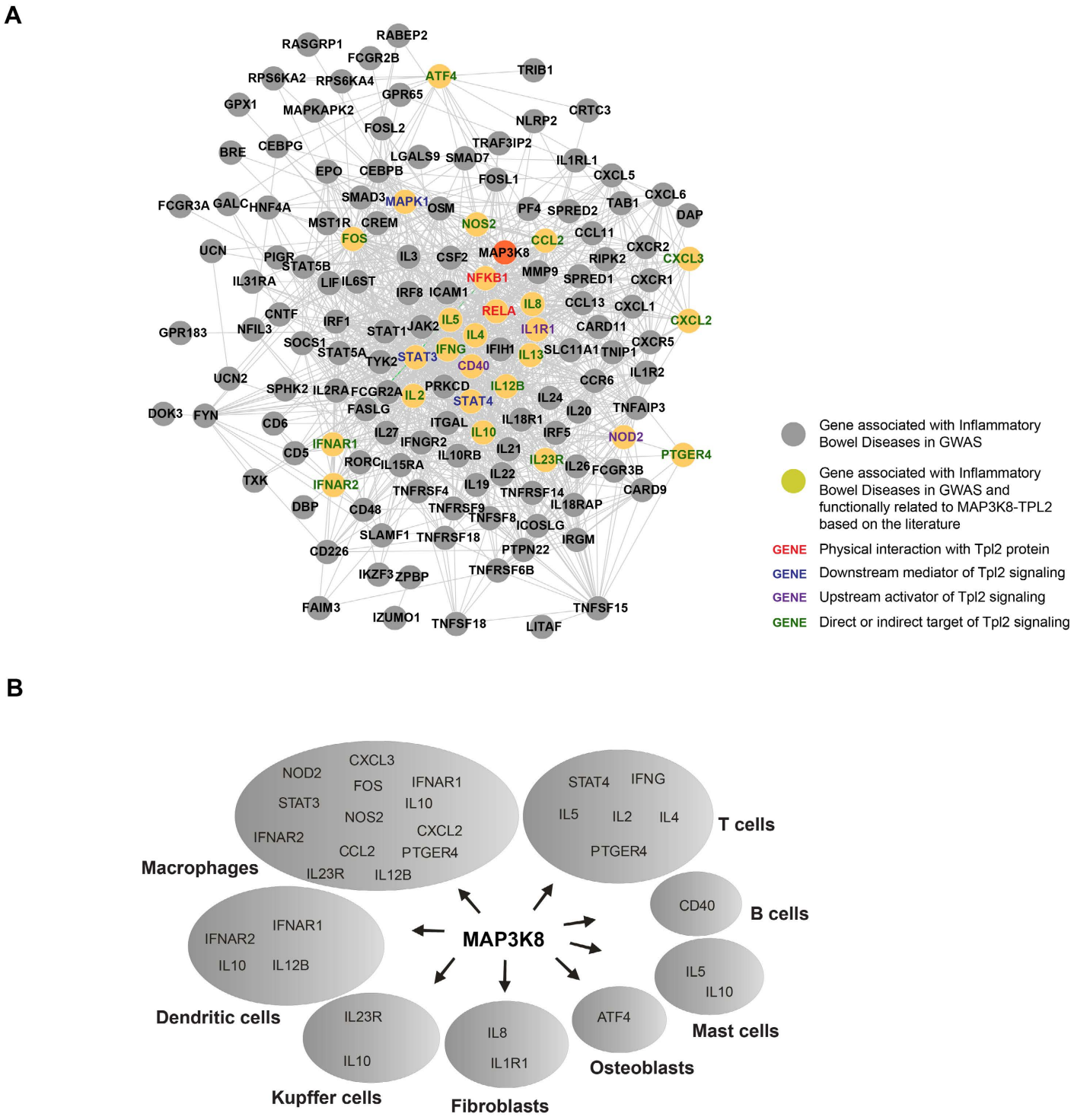

Figure S2

***MAP3K8* is functionally connected to 26 out of 163 IBD-associated genes through physical (2/26) or signaling (24/26) interaction in a wide spectrum of cell types.**

(*A*) Network of IBD-associated genes in GWAS (40) in which a *MAP3K8* functional sub-network is indicated. The IBD-GWAS network was established importing genes associated with IBD (GRAIL $P<0.05$) (40) in the STRING v9.0 database software (13). Genes functionally related to *MAP3K8* were manually identified by literature search for experimental evidence (see Table S1). Network visualization was performed using Cytoscape v2.8.3 software (14, 42).

(*B*) Analysis of cellular specificities of the connections between *MAP3K8* and other IBD-associated genes based on the literature (see Table S1) reveals a wide spectrum of cellular pathways relevant to IBD pathogenesis which could involve *MAP3K8*.

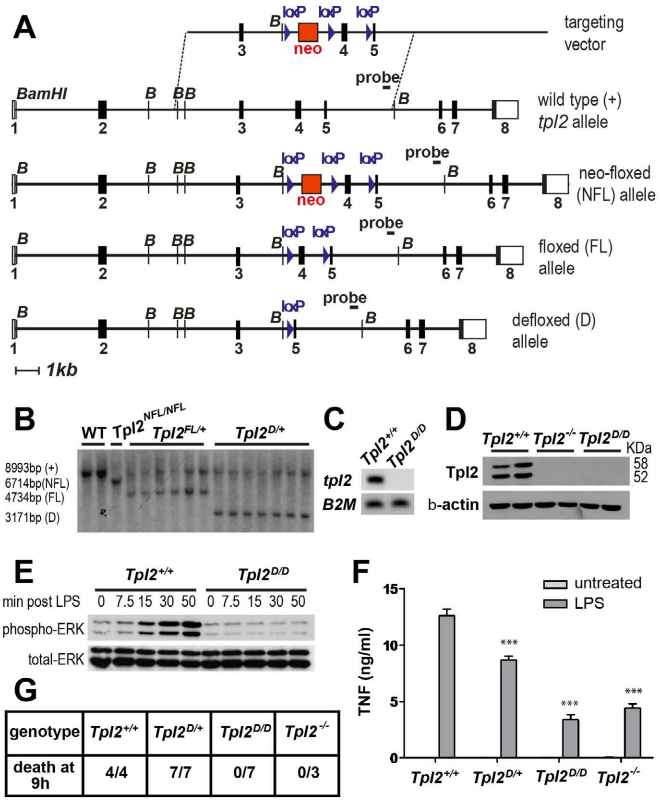

genotype	$Tpl2^{+/+}$	$Tpl2^{D/+}$	$Tpl2^{D/D}$	$Tpl2^{-/-}$
death at 9h	4/4	7/7	0/7	0/3

Figure S3

Generation and characterization of *tpl2* (*map3k8*) conditional knockout mice.

(*A*) Schematic representation of the targeting strategy for the *tpl2* gene. Neo represents a neomycin cassette. White and black boxes represent respectively non-coding and coding sequences of *tpl2* exons. BamHI restriction sites are indicated with *B*. A detailed description of the targeting strategy is included in methods.

(*B*) $Tpl2^{FL/+}$ and $Tpl2^{D/+}$ mice were generated by *Ella-Cre*-mediated genetic recombinations in $Tpl2^{NFL/NFL}$ mice. The recombinations were validated by Southern blot analysis in BamHI digested genomic DNA.

(*C-D*) *tpl2* inactivation in $Tpl2^{D/D}$ mice was validated at the gene expression level with RT-PCR for exon 4 in tissues (*C*), and at the protein level with western blot in macrophages (*D*). $Tpl2^{-/-}$ mice (4) were used as control.

(*E-F*) Total exudate peritoneal macrophages from $Tpl2^{D/D}$ mice show defective ERK activation after stimulation with LPS (*E*) and defective TNF secretion 6 hours after stimulation as shown by ELISA (*F*). Data represent mean ± SEM. (*** $P < 0.001$; Student's t-test).

(*G*) $Tpl2^{D/D}$ mice are resistant to the TNF-dependent LPS/D-galactosamine-induced lethal endotoxic shock. $Tpl2^{-/-}$ mice (4) were used as controls.

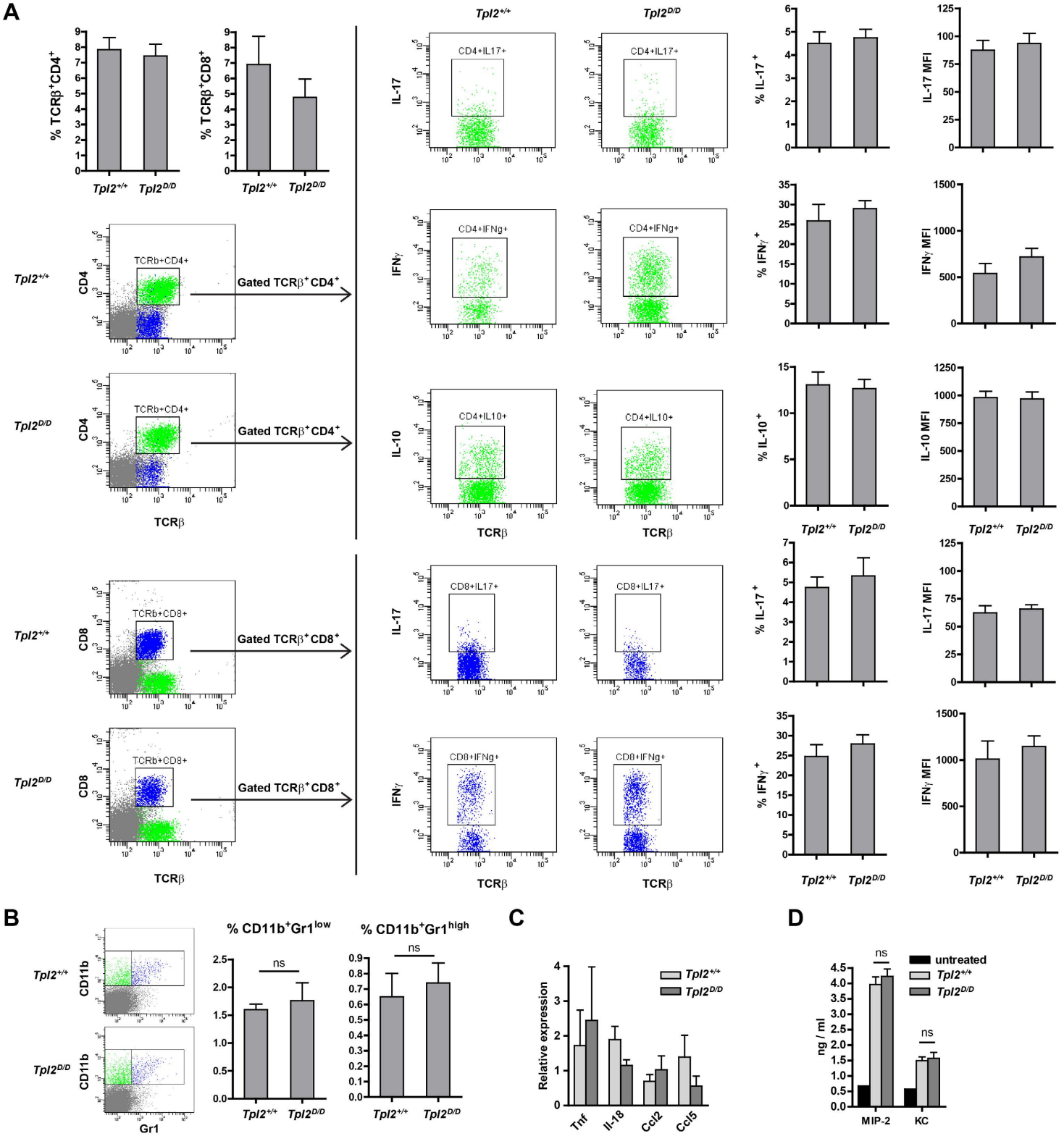

Figure S4

The absence of Tpl2 does not affect adaptive immune responses in the lamina propria, the infiltration of innate immune effectors in the mesenteric lymph nodes and the expression of several inflammatory mediators in the colon upon DSS treatment.

(*A*) Colonic lamina propria cells were isolated from *Tpl2*$^{D/D}$ mice (n=5) and WT littermate controls (n=5) on day 3 upon DSS treatment, stimulated with PMA/Ionomycin and analyzed by flow cytometry for intracellular cytokine expression. No significant differences were observed in the infiltration of TCRβ^{+}CD4^{+} and TCRβ^{+}CD8^{+} cells in the lamina propria and the expression of IL-17, IL-10 and interferon gamma (IFNγ) either as a percentage of positive cells or in terms of Mean Fluorescence Intensity (MFI).

(*B*) Mesenteric lymph node cells were isolated from *Tpl2*$^{D/D}$ mice (n=5) and WT controls (n=6) on day 3 upon DSS treatment and analyzed by flow cytometry for the quantification of macrophages (CD11b^{+}Gr1^{low}) and granulocytes (CD11b^{+}Gr1^{hi}).

(*C*) Expression levels of Tnf, IL-18, Ccl2 (MCP-1) and Ccl5 (RANTES) were determined by quantitative RT-PCR analysis in the terminal colon of *Tpl2*$^{D/D}$ mice and WT controls on day 3 upon DSS treatment. No significant differences were observed.

(*D*) Levels of MIP-2 (Cxcl2) and KC (Cxcl1) were determined by ELISA in colon culture supernatants from *Tpl2*$^{D/D}$ and WT control mice treated with DSS for 5 days.

All data shown represent mean ± SEM. Statistical significance was calculated with Student's t-test (ns, nonsignificant)

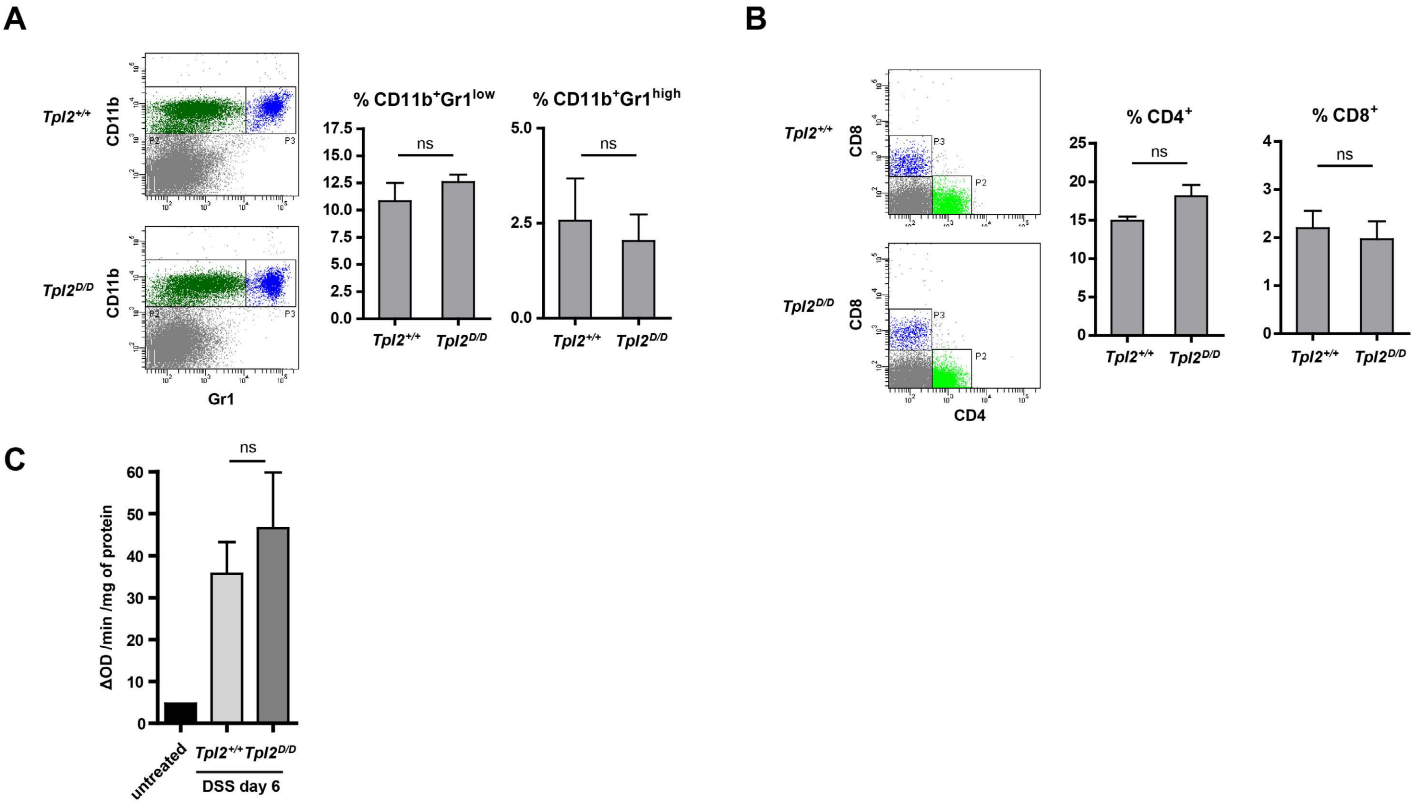

Figure S5

Tpl2 is dispensable for the development of inflammatory responses in the lamina propria on day-6 upon DSS treatment.

(*A-B*) Colonic lamina propria cells were isolated from *Tpl2*$^{D/D}$ mice (n=3) and WT littermate controls (n=3) on day 6 upon DSS treatment. (*A*) Quantification of macrophages (CD11b^{+}Gr1^{low}) and granulocytes (CD11b^{+}Gr1^{hi}) by flow cytometry analysis.

(*B*) Quantification of CD4^{+} and CD8^{+} T-lymphocytes by flow cytometry analysis.

(*C*) *Tpl2*$^{D/D}$ mice (n=5) and WT controls (n=5) show similar myeloperoxidase activity in the colon on day 6 of DSS treatment.

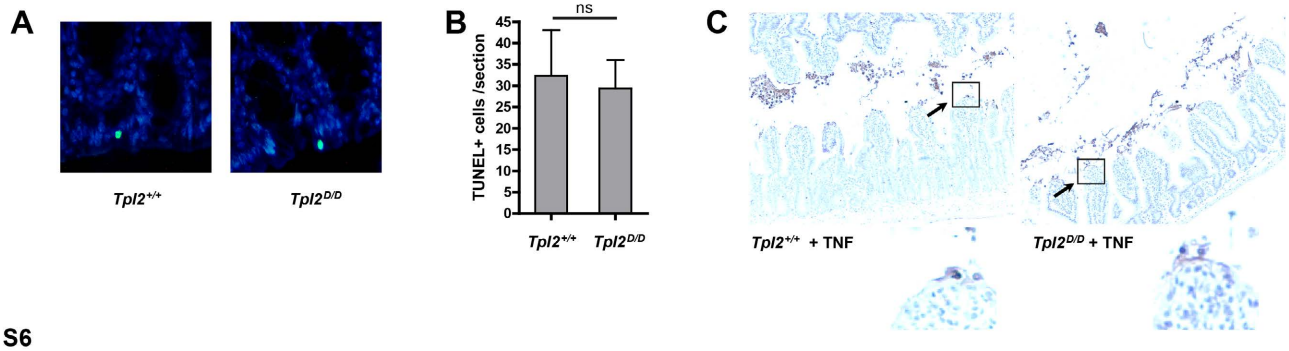

Figure S6

The absence of Tpl2 does not affect the extent of epithelial cell death upon DSS treatment and does not sensitize intestinal epithelial cells to TNF.

(*A*) The extent of epithelial apoptosis was examined in DSS-treated *Tpl2*$^{D/D}$ and WT control mice on experimental days 3 and 5 with TUNEL assays. Indicative photomicrographs are shown. Magnification x200.

(*B*) Quantification of TUNEL assays performed in DSS-treated mice (day 5). Data shown represent mean ± SEM. Statistical significance was calculated with Student's t-test (ns, nonsignificant)

(*C*) *Tpl2*$^{D/D}$ mice and WT controls were injected i.v. with 12 μg murine recombinant TNF and sacrificed 1 hour later. To examine the extent of TNF-induced epithelial cell death TUNEL assays were performed in paraffin sections of the terminal ileum. Magnification x100. Black arrows indicate examples of apoptotic intestinal epithelial cells detaching to the lumen.

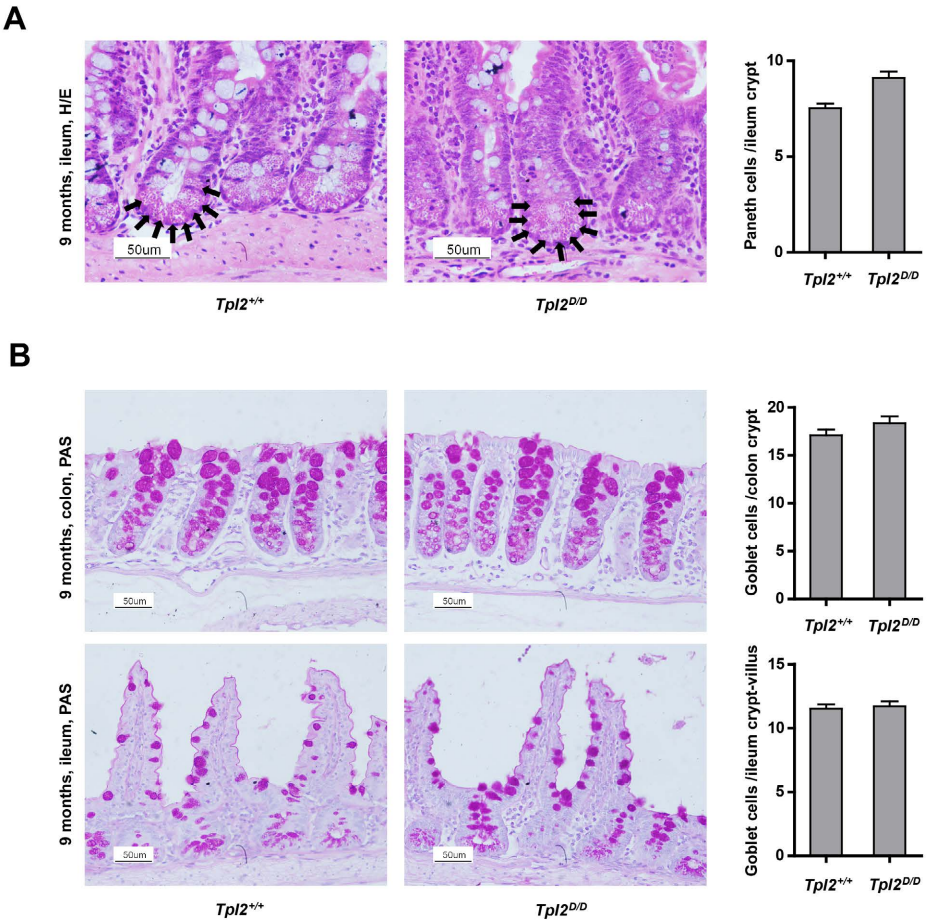

Figure S7

***Tpl2*$^{D/D}$ mice show normal Paneth and Goblet cell populations in the terminal ileum and the colon at the age of 9 months, indicative of unaffected epithelial differentiation mechanisms.**

(*A*) Paneth cell numbers are not affected by Tpl2 ablation. Paneth cells were quantified in H/E-stained sections of the terminal ileum of 9 month-old *Tpl2*$^{D/D}$ mice (n=3) and WT controls (n=3) in at least n=40 well-oriented crypts per genotype.

(*B*) Goblet cell numbers are not affected by Tpl2 ablation. Goblet cells were quantified in Periodic acid-Schiff (PAS)-stained sections of the terminal ileum and the colon of 9 month-old *Tpl2*$^{D/D}$ mice (n=3) and WT controls (n=3) in at least n=50 well-oriented crypt-villus axes and n=20 crypts respectively.

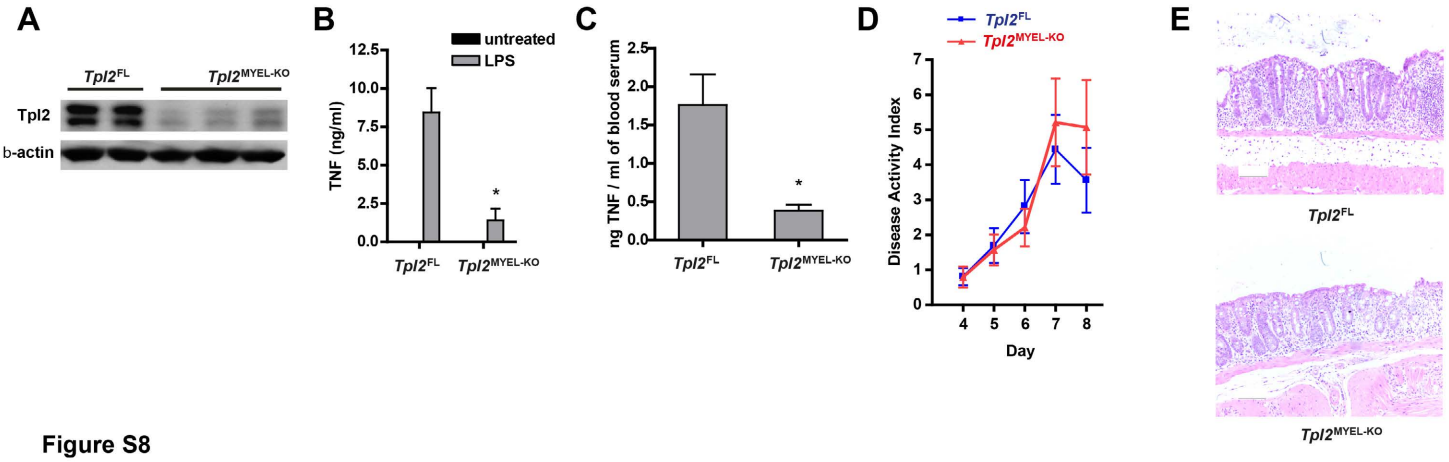

Figure S8

Characterization, Disease Activity Index and histopathology of *Tpl2*$^{MYEL-KO}$ mice.

(*A*) Western blot for the detection of Tpl2 protein expression in macrophages from *Tpl2*$^{MYEL-KO}$ and *Tpl2*^{FL} control mice.

(*B*) Total exudate peritoneal macrophages isolated from *Tpl2*$^{MYEL-KO}$ and *Tpl2*^{FL} mice were examined for TNF secretion after LPS stimulation by ELISA.

(*C*) *Tpl2*$^{MYEL-KO}$ (n=4) and *Tpl2*^{FL} (n=5) control mice were injected i.p. with 100 µg LPS and serum samples were collected 90 min later. The levels of TNF in the serum were determined by ELISA.

(*D*) Disease Activity Index of *Tpl2*$^{MYEL-KO}$ (n= 14) and *Tpl2*^{FL} control mice (n=16) treated with 2.5% DSS in two independent experiments. No significant differences were observed.

(*E*) Colon sections from DSS-treated *Tpl2*$^{MYEL-KO}$ (n= 14) and *Tpl2*^{FL} control mice (n=16) sacrificed on experimental day 8 were stained with H&E for histological examination. (Scale bars: 100 µm.)

All data shown represent mean ± SEM. Statistical significance was calculated with Student's t-test (* $P < 0.05$; ns, nonsignificant)

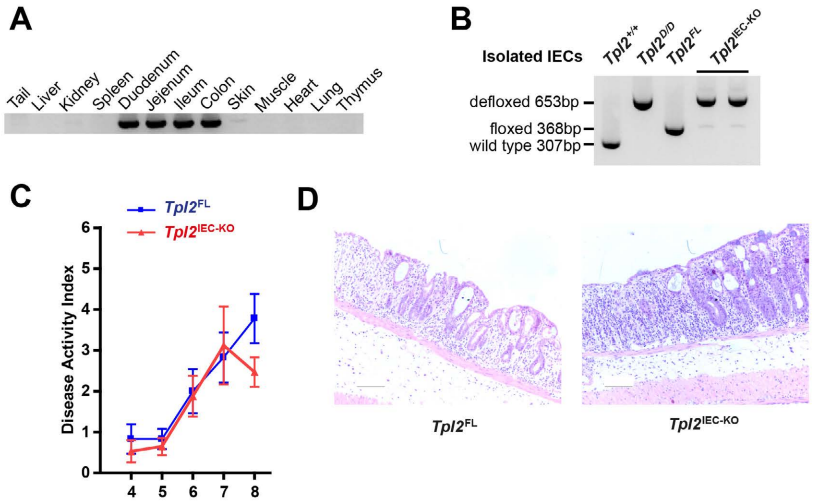

Figure S9

Characterization, Disease Activity Index and histopathology of *Tpl2*$^{IEC-KO}$ mice.

(*A*) PCR analysis in tissues from *Tpl2*$^{IEC-KO}$ mice showing that the *VillinCre*-mediated recombination producing the defloxed tpl2 allele occurs specifically in the intestine.

(*B*) PCR analysis in isolated intestinal epithelial cells from the colon of *Tpl2*$^{IEC-KO}$ and *Tpl2*^{FL}, *Tpl2*$^{+/+}$ and *Tpl2*$^{D/D}$ control mice showing the efficiency of the *VillinCre*-mediated recombination producing the defloxed tpl2 allele in intestinal epithelial cells.

(*C*) Disease Activity Index of *Tpl2*$^{IEC-KO}$ (n= 17) and *Tpl2*^{FL} control mice (n=18) treated with 2.5% DSS in three independent experiments. Data shown represent mean ± SEM. Statistical significance was calculated with Student's t-test. No significant differences were observed.

(*D*) Colon sections from DSS-treated *Tpl2*$^{IEC-KO}$ (n= 6) and *Tpl2*^{FL} control mice (n=7) sacrificed on experimental day 8 were stained with H&E for histological examination. (Scale bars: 100 µm.)

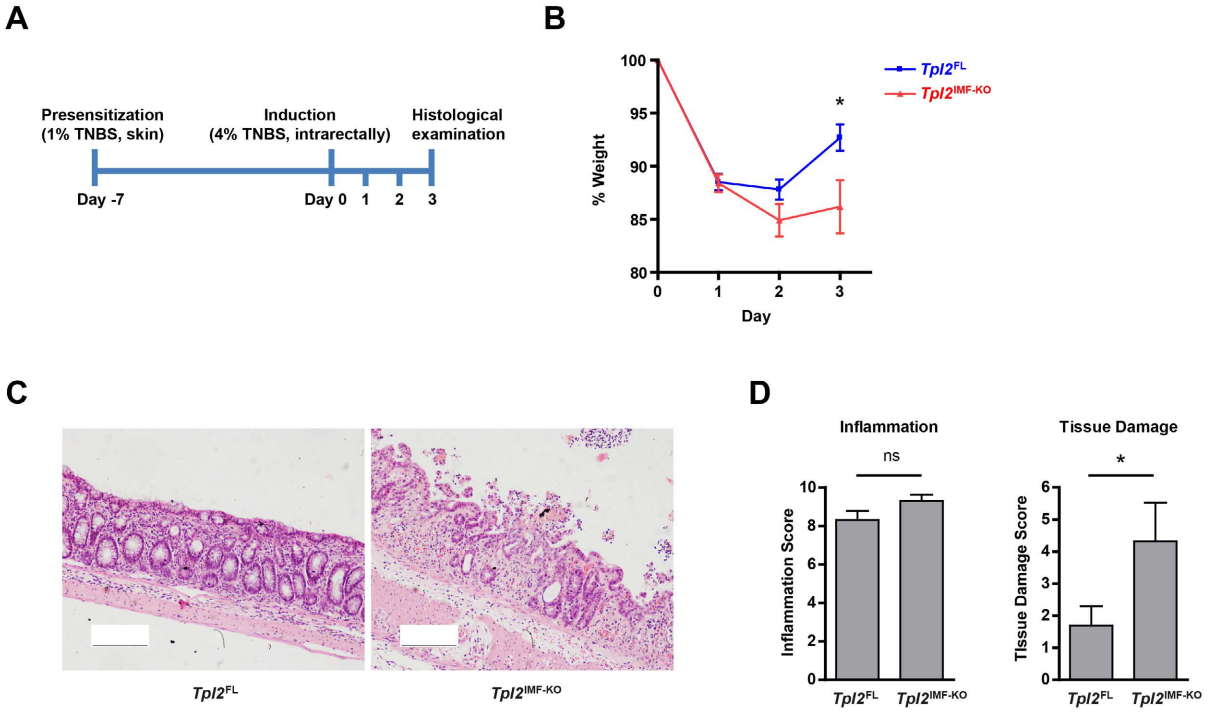

Figure S10

Tpl2 in intestinal myofibroblasts protects from TNBS-induced colitis.

(*A*) *Tpl2*$^{IMF\text{-}KO}$ (n= 9) and *Tpl2*^{FL} control mice (n= 8) were pre-sensitized to TNBS on day -7 by applying a 1% TNBS solution on the skin as described in Methods. Colitis was induced on day 0 by intrarectal instillation of a 4% TNBS solution in 40% ethanol.

(*B*) *Tpl2*$^{IMF\text{-}KO}$ mice show significantly increased weight loss on day 3 upon induction of TNBS colitis as compared to *Tpl2*^{FL} controls. Data shown represent mean ± SEM. Statistical significance was calculated with Student's t-test (* $P < 0.05$).

(*C*) *Tpl2*$^{IMF\text{-}KO}$ mice show exacerbated tissue damage on day 3 upon TNBS induction, characterized by enhanced loss of crypts and disruption of the epithelial integrity. Representative photomicrographs are shown. H&E-stained sections. (Scale bars: 100 µm.)

(*D*) *Tpl2*$^{IMF\text{-}KO}$ mice show significantly increased tissue damage score and similar inflammation score on day 3 upon induction of TNBS colitis as compared to *Tpl2*^{FL} controls. Data shown represent mean ± SEM. Statistical significance was calculated with Mann-Whitney test (* $P < 0.05$; ns, nonsignificant).

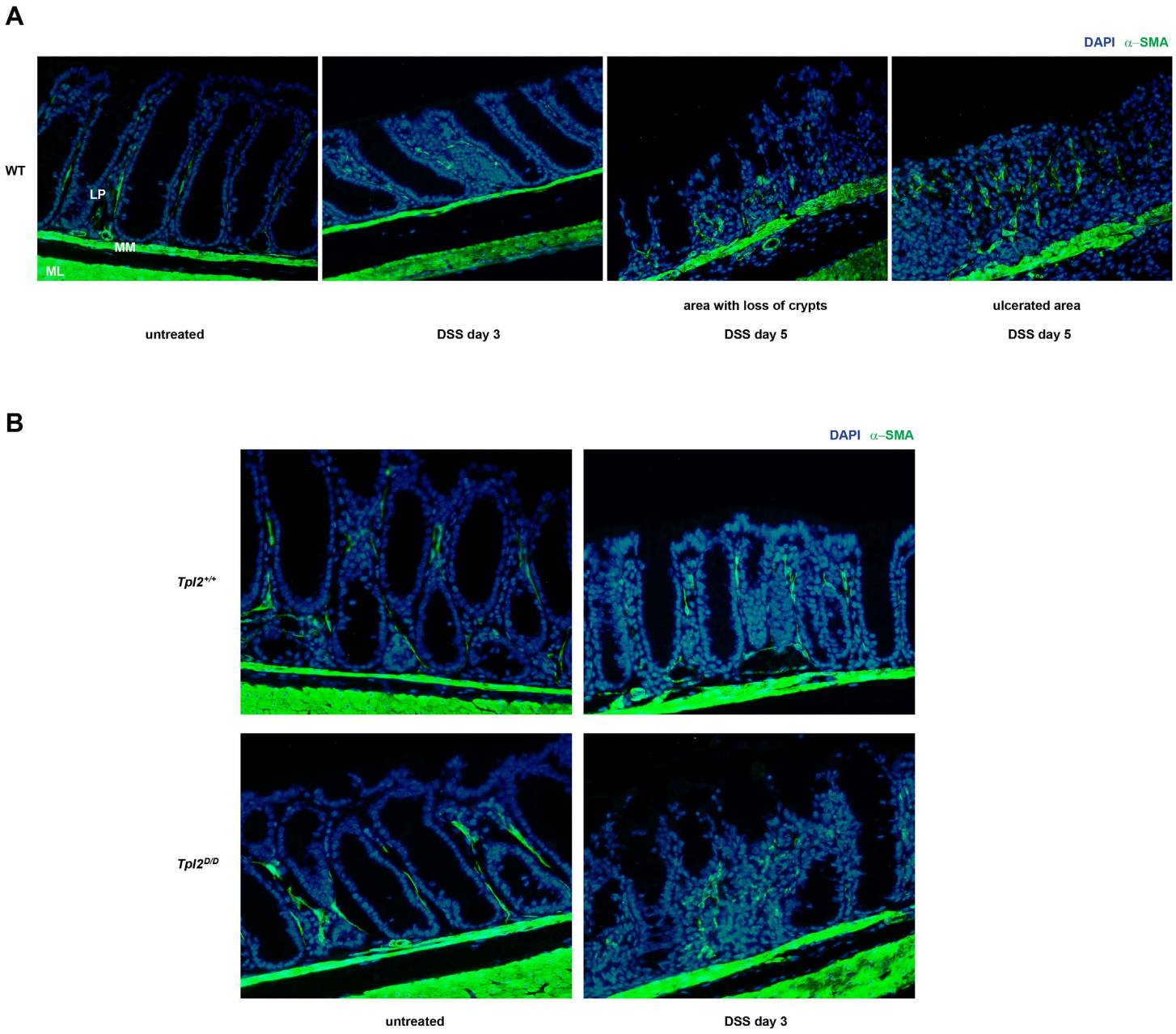

Figure S11

The network of mesenchymal cells in the lamina propria is reorganized in response to DSS-induced epithelial injury.

(*A*) Normal mice were treated with 2.5% days for 3 or 5 days. Paraffin sections of the colon were stained for α-SMA, a cytoskeletal protein expressed by smooth muscle cells of the muscular layer (ML) and the muscularis mucosae (MM) and by myofibroblasts, lymphatic lacteal-associated smooth muscle cells and pericytes of the lamina propria (LP). The network of α-SMA^{+} mesechymal cells in the lamina propria is reorganized in damaged areas of the colon.

(*B*) *Tpl2*$^{D/D}$ mice and WT controls were treated with 2.5% days for 3 days. Paraffin sections of the colon were stained for α-SMA. Nuclei are stained with DAPI. (Magnification x 200).

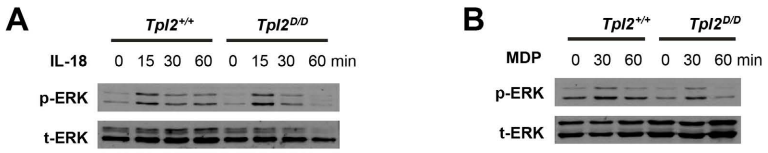

Figure S12

Tpl2 in intestinal myofibroblasts does not mediate ERK activation by NOD2 or IL-18R stimulation.

IMFs isolated from *Tpl2*$^{D/D}$ and WT control mice were stimulated with (*A*) IL-18 or (*B*) muramyl dipeptide (MDP) for the time-points indicated. Western blots for phospho-ERK (p-ERK) were performed. Total ERK (t-ERK) was used as a loading control.

A

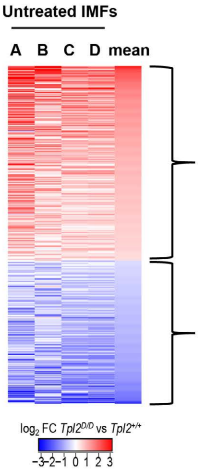

n=244 genes overexpressed in *Tpl2*$^{D/D}$ IMFs

Transcription Factors predicted	Enrichr Combined Score	WebGestalt Adjusted *P*-value
MYOG	16.542	7.00E-04
MYOD1	10.233	8.48E-07
EGR1	10.011	1.00E-03
SP1	4.364	1.63E-10

n=179 genes underexpressed in *Tpl2*$^{D/D}$ IMFs

Transcription Factors predicted	Enrichr Combined Score	WebGestalt Adjusted *P*-value
SREBP1	5.703	1.00E-03
AP1 (JUN/FOS)	5.608	4.40E-03
CREB1	4.896	2.00E-04

B

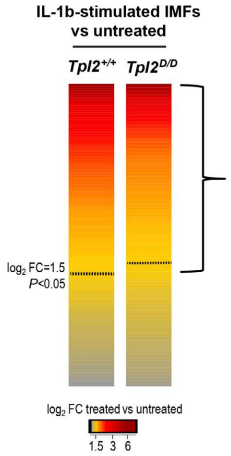

IL-1b-induced genes in *Tpl2*$^{+/+}$ IMFs

Transcription Factors predicted	Enrichr Combined Score	WebGestalt Adjusted *P*-value
NFKB	16.437	1.45E-13
AP1 (JUN/FOS)	12.010	5.19E-09

IL-1b-induced genes in *Tpl2*$^{D/D}$ IMFs

Transcription Factors predicted	Enrichr Combined Score	WebGestalt Adjusted *P*-value
NFKB	21.978	4.26E-14
AP1 (JUN/FOS)	6.488	6.21E-05

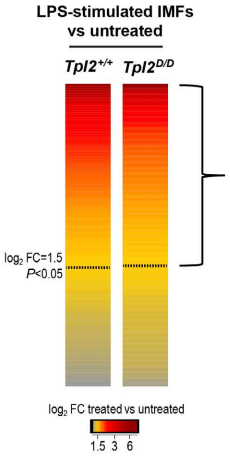

LPS-induced genes in *Tpl2*$^{+/+}$ IMFs

Transcription Factors predicted	Enrichr Combined Score	WebGestalt Adjusted *P*-value
NFKB	18.715	1.45E-13
AP1 (JUN/FOS)	12.802	5.19E-09
STAT5B	5.655	4.49E-05
IRF8	4.566	1.90E-03

LPS-induced genes in *Tpl2*$^{D/D}$ IMFs

Transcription Factors predicted	Enrichr Combined Score	WebGestalt Adjusted *P*-value
NFKB	20.257	1.42E-11
AP1 (JUN/FOS)	4.094	3.20E-03

Figure S13

Inference of transcription factors from the gene expression profile of IMFs isolated from *Tpl2*$^{D/D}$ and WT control mice.

(*A*) Transcription factors inferred from genes up- or down-regulated in untreated Tpl2$^{D/D}$ IMFs. A list of n=423 genes consistently deregulated in untreated Tpl2$^{D/D}$ IMFs in four independent experiments was used as input for two different algorithms identifying transcription factor enrichments based on experimentally validated binding motifs (Enrichr (16) and WebGestalt (17), see Methods). Transcription factors predicted by both algorithms with an adjusted *P*-value < 0.05 are shown.

(*B*) Transcription factors inferred from genes induced by IL-1β or LPS in Tpl2$^{+/+}$ and Tpl2$^{D/D}$ IMFs. Genes induced by IL-1β or LPS with a $\log_2$ Fold Change threshold ($\log_2$ FC) = 1.5 and *P*-value < 0.05 were used as input for transcription factor binding motif enrichment as above. Transcription factors predicted by both algorithms with an adjusted *P*-value < 0.05 in two independent experiments are shown.

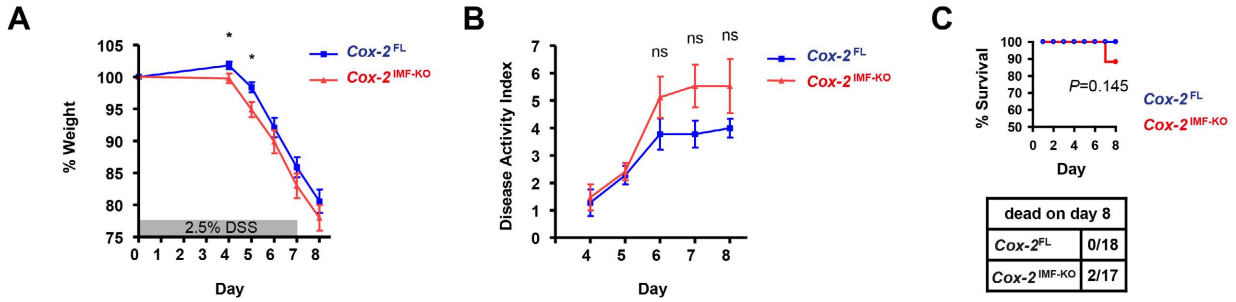

Figure S14

Cox-2 ablation in intestinal myofibroblasts leads to increased susceptibility to DSS-induced colitis in the early phase of the protocol.

Cox-2^{IMF-KO} (n= 17) and *Cox-2*^{FL} control mice (n=18) were treated with 2.5% DSS in three independent experiments.

(*A*) *Cox-2*$^{IMF-KO}$ mice show increased weight loss in the early phase of the DSS-induced colitis protocol.

(*B*) Disease Activity Index calculations in the same experiments show no statistically significant differences.

(*C*) Lethality data in the same experiments (*P* = 0.145; Gehan-Wilcoxon test).

All data represent mean ± SEM. Student's t-test (* *P* < 0.05; ns, nonsignificant)

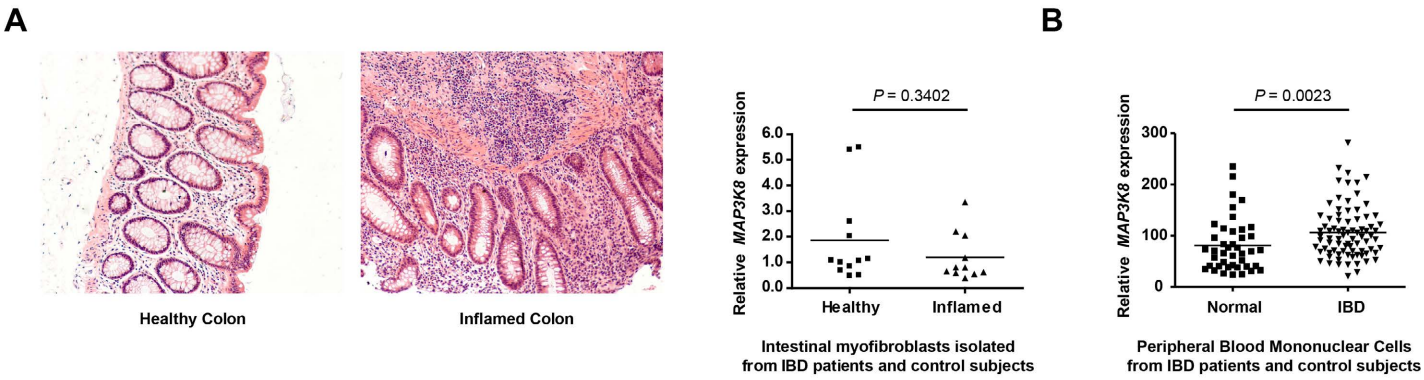

Figure S15

***MAP3K8* expression in IMFs isolated from the colon and Peripheral Blood Mononuclear Cells of IBD patients.**

(*A*) IMFs were isolated from healthy and inflamed colon tissues of IBD patients (n=11) and from healthy tissues of additional control subjects (n=4). (see Methods for clinical data). Indicative photomicrographs of H&E-stained sections of colonic biopsies from these patients are shown. (Magnification x 100). *MAP3K8* gene expression levels were measured by RT-PCR. Data shown represent mean ± SEM. Mann-Whitney test.

(*B*) *MAP3K8* expression is slightly increased in Peripheral Blood Mononuclear Cells of IBD patients (n=83) as compared to normal subjects (n=42). Data were retrieved from the Gene Expression Omnibus database (GEO ID 16705254) (43). Data shown represent mean ± SEM. Statistical significance was calculated by Mann-Whitney test.

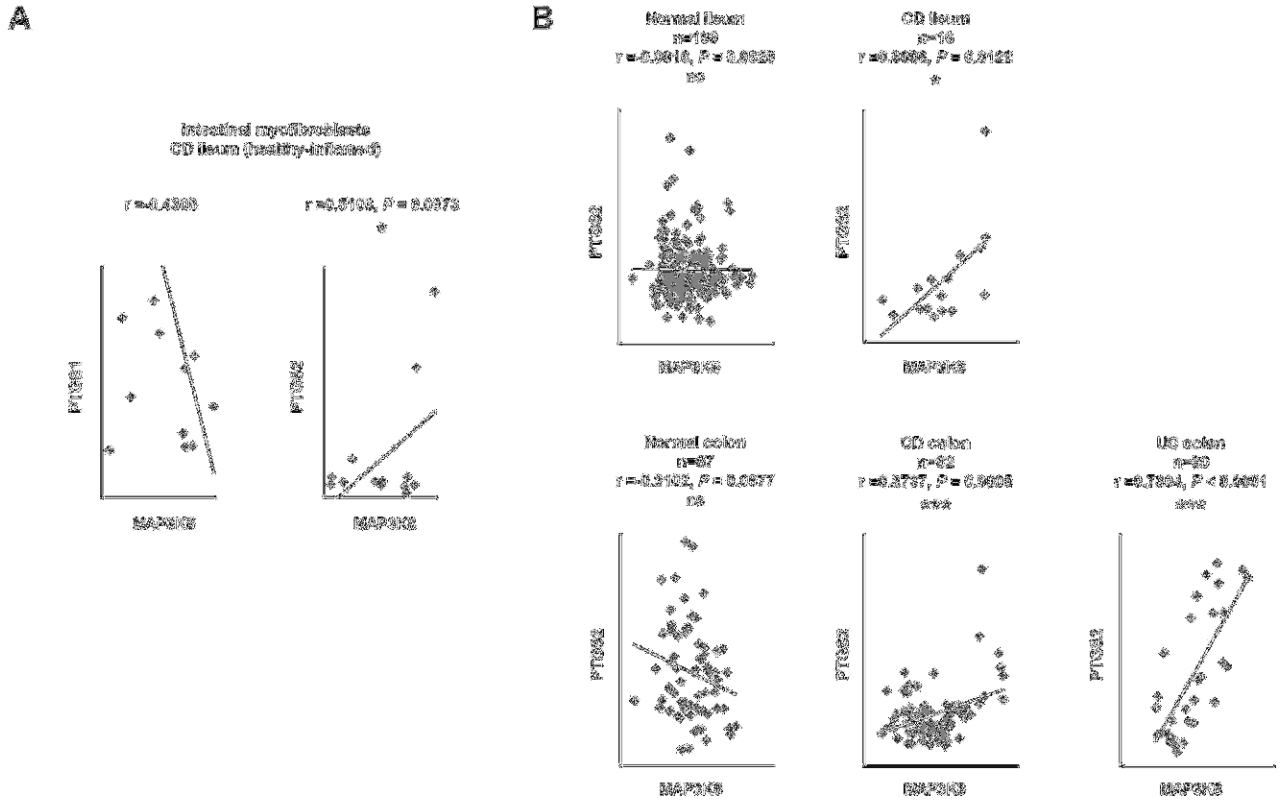

Figure S16

Comparison of *MAP3K8* and *PTGS2* gene expression levels in isolated IMFs and biopsies from IBD patients and control subjects.

(*A*) IMFs were isolated from inflamed (n=7) or healthy (n=6) ileal tissues of patients suffering from Crohn's disease. *MAP3K8*, *PTGS1* and *PTGS2* gene expression levels were measured by RT-PCR. Pearson correlation coefficient and one-tailed *P*-value were computed to assess whether *MAP3K8* gene expression positively correlates with *PTGS2* expression. Correlation between *MAP3K8* and *PTGS2*, but not *PTGS1*, gene expression levels is observed in cultured IMFs.

(*B*) *MAP3K8* gene expression positively correlates with *PTGS2* gene expression in intestinal biopsies from patients suffering from IBD but not from healthy control subjects. Data were retrieved from the Gene Expression Omnibus database (GEO datasets: GSE40282 for the healthy ileum (44), GSE20881 for CD ileum, CD colon and healthy colon (45) and GSE38713 for UC colon (46)). Pearson correlation coefficient and two-tailed *P*-value were computed to assess any potential correlation between *MAP3K8* and *PTGS2*. (* $P < 0.05$; *** $P < 0.001$; ns, nonsignificant)

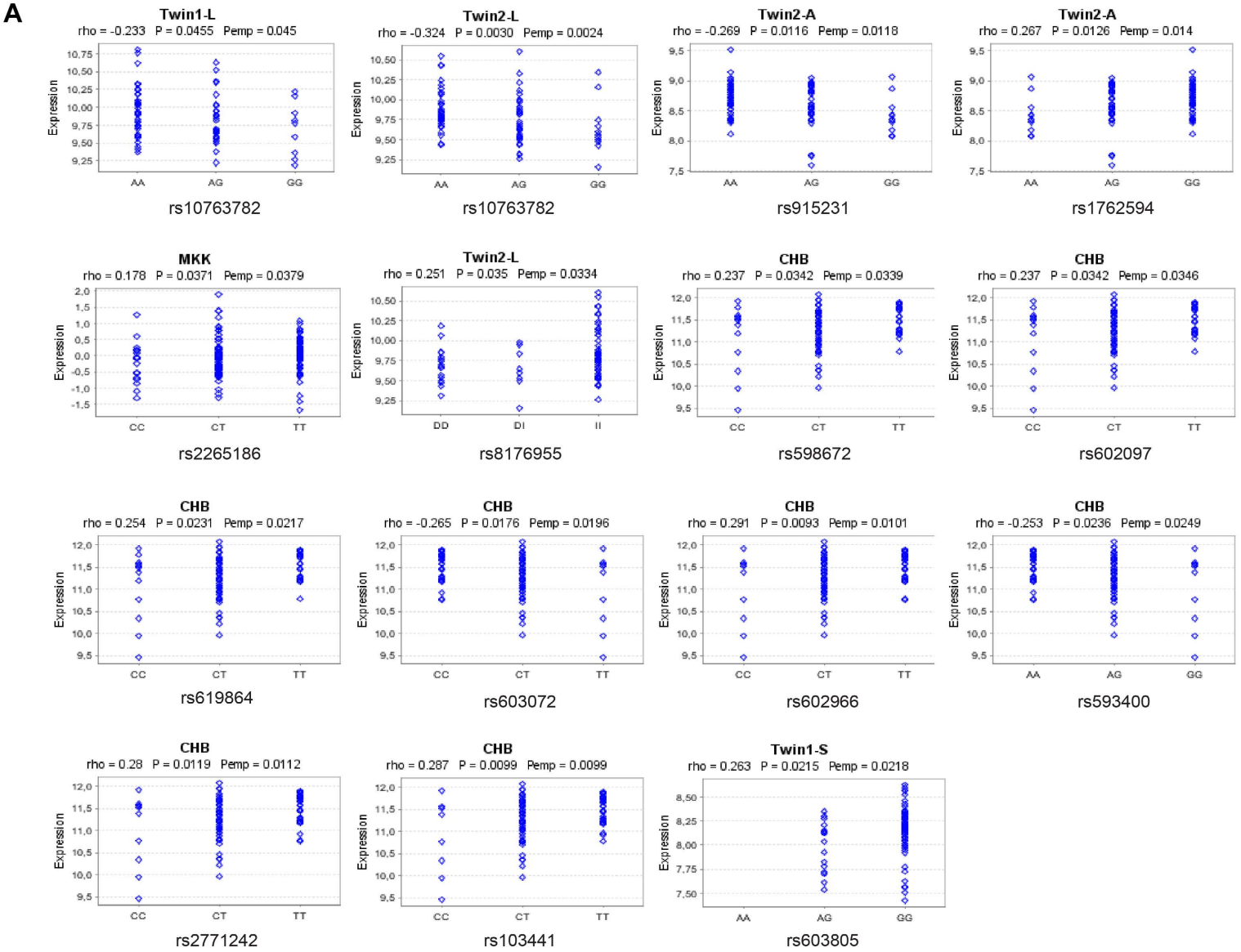
A
Twin1-L
rho = -0.233 P = 0.0455 Pemp = 0.045
rs10763782
Twin2-L
rho = -0.324 P = 0.0030 Pemp = 0.0024
rs10763782
Twin2-A
rho = -0.269 P = 0.0116 Pemp = 0.0118
rs915231
Twin2-A
rho = 0.267 P = 0.0126 Pemp = 0.014
rs1762594
MKK
rho = 0.178 P = 0.0371 Pemp = 0.0379
rs2265186
Twin2-L
rho = 0.251 P = 0.035 Pemp = 0.0334
rs8176955
CHB
rho = 0.237 P = 0.0342 Pemp = 0.0339
rs598672
CHB
rho = 0.237 P = 0.0342 Pemp = 0.0346
rs602097
CHB
rho = 0.254 P = 0.0231 Pemp = 0.0217
rs619864
CHB
rho = -0.265 P = 0.0176 Pemp = 0.0196
rs603072
CHB
rho = 0.291 P = 0.0093 Pemp = 0.0101
rs602966
CHB
rho = -0.253 P = 0.0236 Pemp = 0.0249
rs593400
CHB
rho = 0.28 P = 0.0119 Pemp = 0.0112
rs2771242
CHB
rho = 0.287 P = 0.0099 Pemp = 0.0099
rs103441
Twin1-S
rho = 0.263 P = 0.0215 Pemp = 0.0218
rs603805
Expression
CC
CT
TT
AA
AG
GG
DD
DI
II

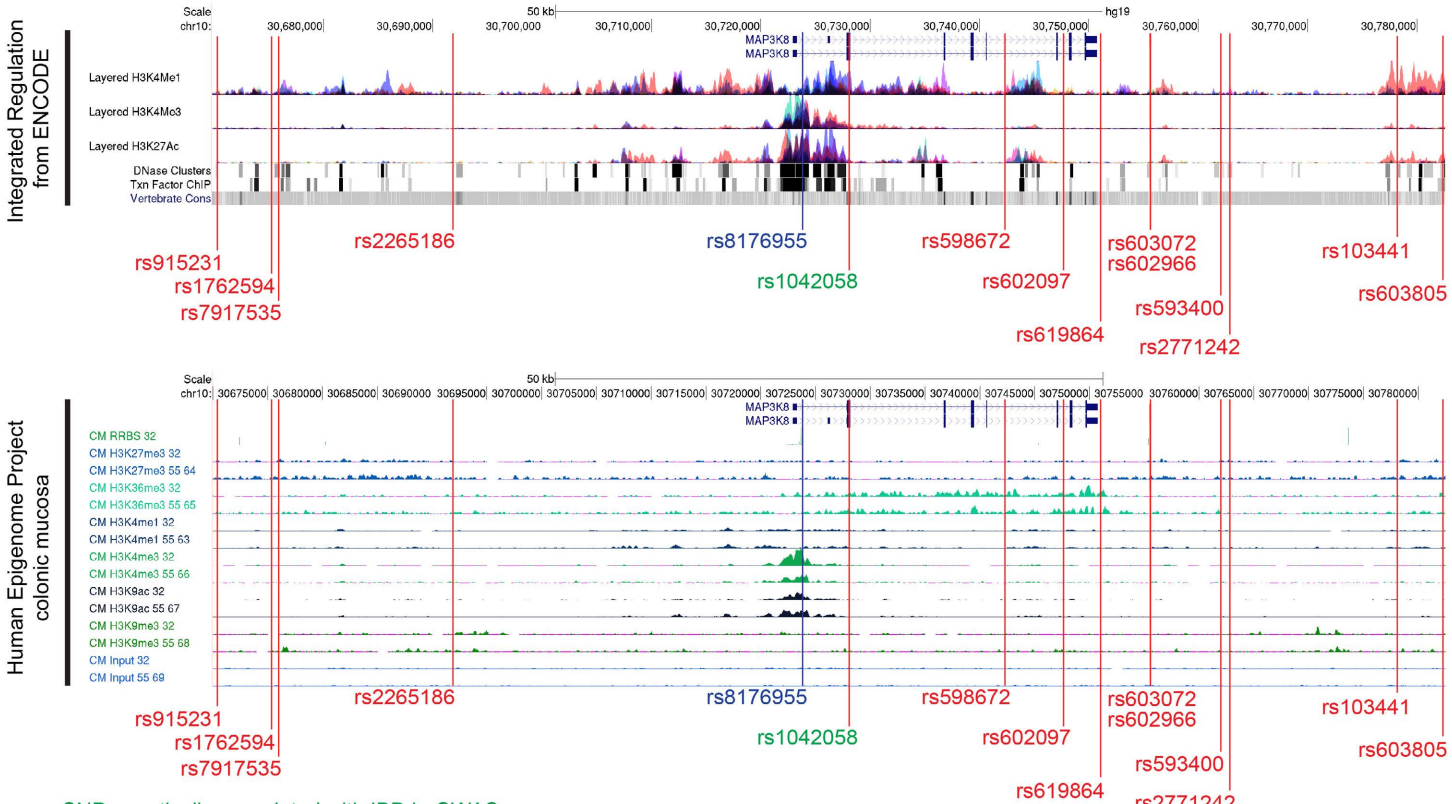
B
Integrated Regulation from ENCODE
Scale
chr10:
50 kb
hg19
MAP3K8
Layered H3K4Me1
Layered H3K4Me3
Layered H3K27Ac
DNase Clusters
Txn Factor ChIP
Vertebrate Cons
rs915231
rs1762594
rs7917535
rs2265186
rs8176955
rs1042058
rs598672
rs602097
rs619864
rs603072
rs602966
rs593400
rs2771242
rs103441
rs603805
Human Epigenome Project colonic mucosa
CM RRBS 32
CM H3K27me3 32
CM H3K27me3 55 64
CM H3K36me3 32
CM H3K36me3 55 65
CM H3K4me1 32
CM H3K4me1 55 63
CM H3K4me3 32
CM H3K4me3 55 66
CM H3K9ac 32
CM H3K9ac 55 67
CM H3K9me3 32
CM H3K9me3 55 68
CM Input 32
CM Input 55 69
SNP genetically associated with IBD in GWAS
SNP whose minor allele is associated with reduced MAP3K8 expression
Deletion whose minor allele is associated with reduced MAP3K8 expression

Figure S17

eQTL analysis in the *MAP3K8* gene region.

(*A*) *Cis*-eQTL analysis performed in the *MAP3K8* gene region ±50 kb around the transcription start site indicates SNPs whose the minor allele is negatively associated with gene expression levels. Data shown were retrieved through Genevar software (Sanger Institute) from the MuTHER healthy twins study performed in adipose tissue (A), lymphoblastoid cells (L) and skin (S) (47), and the HapMap3 lymphoblastoid cell data from Han Chinese individuals in Beijing, China (CHB) and Maasai individuals in Kinyawa, Kenya (MKK) (48). Spearman's *rho*, nominal *P*-value and permutation *P*-value are shown above each plot.

(*B*) UCSC genome browser displays showing the position of the SNPs (red) and deletions (blue) associated with diminished *MAP3K8* gene expression relevantly to ENCODE's Integrated Regulation data (41) from cell lines and Human Epigenome's Project data from healthy colonic mucosa tissues of two donors.

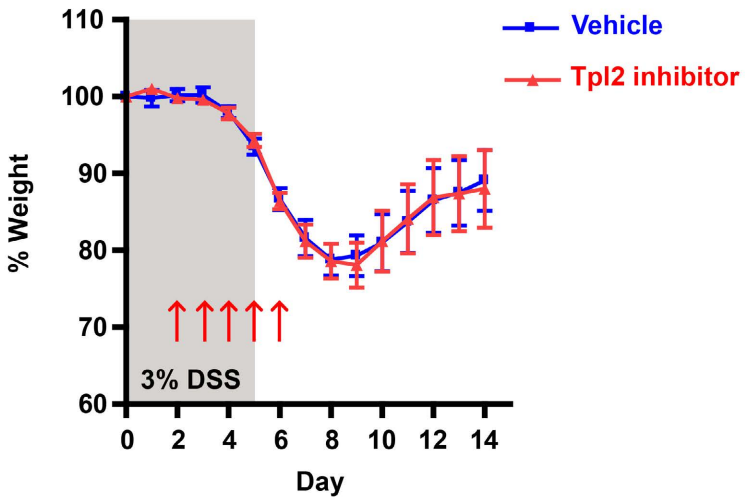

Figure S18

Treatment of WT mice with Tpl2 kinase inhibitor does not affect DSS colitis progression.

C57BL/6J WT mice were treated with 3% DSS receiving intraperitoneally at the time-points indicated Tpl2 kinase inhibitor (Calbiochem #616373, 2.5 mg/kg, dissolved in PBS 2% dimethyl sulfoxide) or vehicle (PBS 2% dimethyl sulfoxide) in two independent experiments (n=8 mice per treatment). The genetic background of the mice, the DSS colitis protocol applied, the dosage and the time-points of Tpl2 inhibitor administration were the same as described by Lawrenz et al (49). All mice used were littermates, sex-matched, sharing the same cages during the experiment independently of the treatment. No significant differences were observed. Data shown represent mean ± SEM.

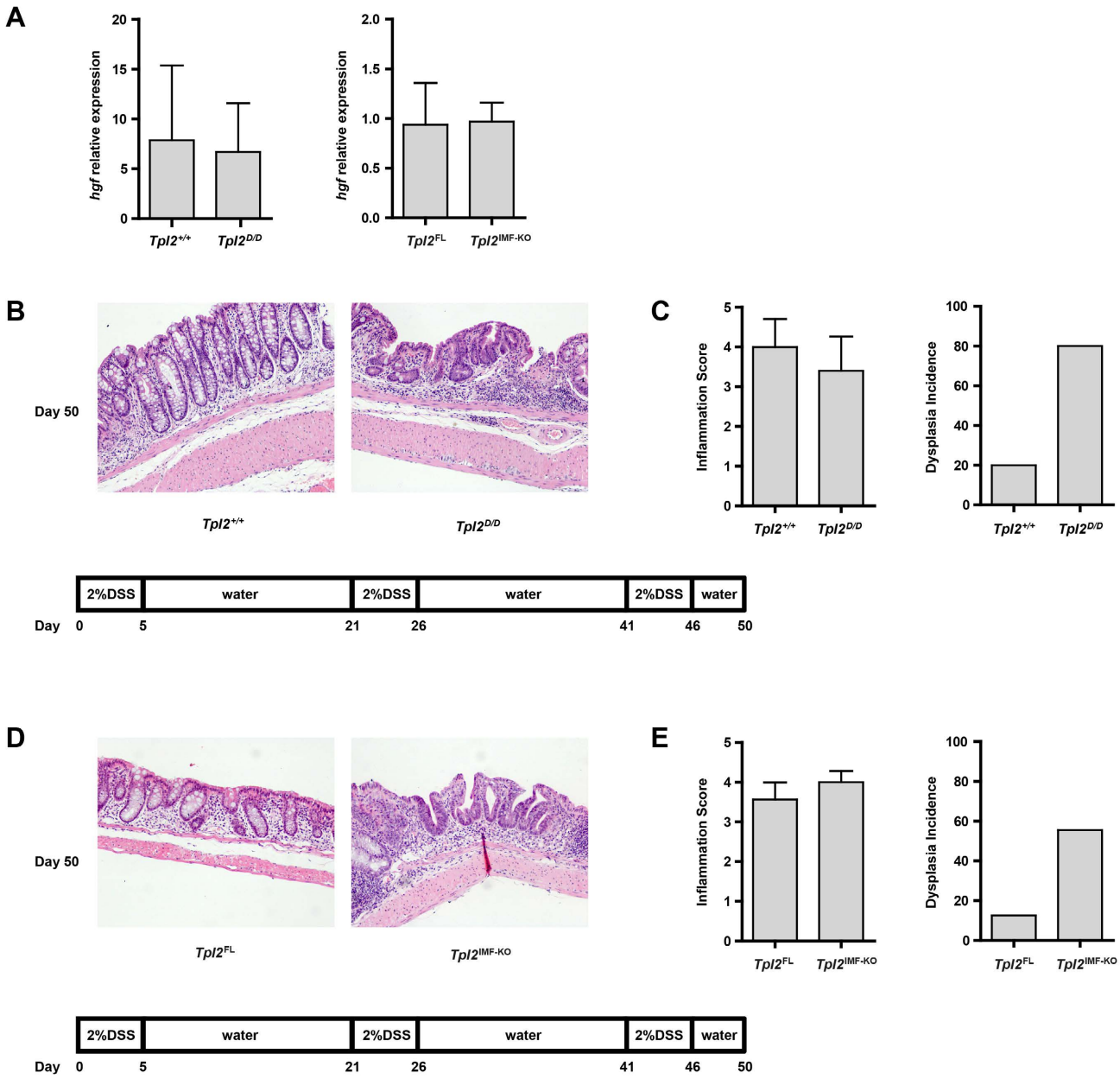

Figure S19

HGF expression and response to chronic DSS treatment in *Tpl2*$^{D/D}$ and *Tpl2*$^{IMF-KO}$ mice.

(*A*) Expression levels of HGF were determined by quantitative RT-PCR analysis in the terminal colon of *Tpl2*$^{D/D}$ mice and WT controls (n=6, each) and *Tpl2*$^{IMF-KO}$ mice and *Tpl2*^{FL} controls (n=4, each) on day 3 upon DSS treatment. No significant differences were observed.

(*B-C*) Chronic colitis was induced in *Tpl2*$^{D/D}$ (*A*) and *Tpl2*$^{IMF-KO}$ (*B*) mice and the respective littermate controls by 2% DSS treatment for 5 consecutive days followed by 16 days of regular drinking water administration. This treatment was repeated to a total number of three cycles. Normal water consumption in the third cycle lasted 4 days. N=6-8 mice/group. Indicative of three independent experiments. All data shown represent mean ± SEM. Magnification x100.

Supplemental references

1. Lakso M, *et al.* (1996) Efficient in vivo manipulation of mouse genomic sequences at the zygote stage. *Proc Natl Acad Sci U S A* 93(12):5860-5865.
2. Armaka M, *et al.* (2008) Mesenchymal cell targeting by TNF as a common pathogenic principle in chronic inflammatory joint and intestinal diseases. *J Exp Med* 205(2):331-337.
3. Ishikawa TO & Herschman HR (2006) Conditional knockout mouse for tissue-specific disruption of the cyclooxygenase-2 (Cox-2) gene. *Genesis* 44(3):143-149.
4. Dumitru CD, *et al.* (2000) TNF-alpha induction by LPS is regulated posttranscriptionally via a Tpl2/ERK-dependent pathway. *Cell* 103(7):1071-1083.
5. Clausen BE, Burkhardt C, Reith W, Renkawitz R, & Forster I (1999) Conditional gene targeting in macrophages and granulocytes using LysMcre mice. *Transgenic Res* 8(4):265-277.
6. Madison BB, *et al.* (2002) Cis elements of the villin gene control expression in restricted domains of the vertical (crypt) and horizontal (duodenum, cecum) axes of the intestine. *J Biol Chem* 277(36):33275-33283.
7. Roulis M, Armaka M, Manoloukos M, Apostolaki M, & Kollias G (2011) Intestinal epithelial cells as producers but not targets of chronic TNF suffice to cause murine Crohn-like pathology. *Proc Natl Acad Sci U S A* 108(13):5396-5401.
8. Shaker A, *et al.* (2010) Epimorphin deletion protects mice from inflammation-induced colon carcinogenesis and alters stem cell niche myofibroblast secretion. *J Clin Invest* 120(6):2081-2093.
9. Koliaraki V, Roulis M, & Kollias G (2012) Tpl2 regulates intestinal myofibroblast HGF release to suppress colitis-associated tumorigenesis. *J Clin Invest* 122(11):4231-4242.
10. Brose SA, Thuen BT, & Golovko MY (2011) LC/MS/MS method for analysis of E(2) series prostaglandins and isoprostanes. *J Lipid Res* 52(4):850-859.
11. Trapnell C, Pachter L, & Salzberg SL (2009) TopHat: discovering splice junctions with RNA-Seq. *Bioinformatics* 25(9):1105-1111.
12. Trapnell C, *et al.* (2010) Transcript assembly and quantification by RNA-Seq reveals unannotated transcripts and isoform switching during cell differentiation. *Nat Biotechnol* 28(5):511-515.
13. Szklarczyk D, *et al.* (2011) The STRING database in 2011: functional interaction networks of proteins, globally integrated and scored. *Nucleic Acids Res* 39(Database issue):D561-568.
14. Shannon P, *et al.* (2003) Cytoscape: a software environment for integrated models of biomolecular interaction networks. *Genome Res* 13(11):2498-2504.
15. Smoot ME, Ono K, Ruscheinski J, Wang PL, & Ideker T (2011) Cytoscape 2.8: new features for data integration and network visualization. *Bioinformatics* 27(3):431-432.
16. Chen EY, *et al.* (2013) Enrichr: interactive and collaborative HTML5 gene list enrichment analysis tool. *BMC Bioinformatics* 14:128.
17. Wang J, Duncan D, Shi Z, & Zhang B (2013) WEB-based GEne SeT AnaLysis Toolkit (WebGestalt): update 2013. *Nucleic Acids Res* 41(Web Server issue):W77-83.
18. Belich MP, Salmeron A, Johnston LH, & Ley SC (1999) TPL-2 kinase regulates the proteolysis of the NF-kappaB-inhibitory protein NF-kappaB1 p105. *Nature* 397(6717):363-368.
19. Bouwmeester T, *et al.* (2004) A physical and functional map of the human TNF-alpha/NF-kappa B signal transduction pathway. *Nat Cell Biol* 6(2):97-105.
20. Eliopoulos AG, Wang CC, Dumitru CD, & Tsichlis PN (2003) Tpl2 transduces CD40 and TNF signals that activate ERK and regulates IgE induction by CD40. *Embo J* 22(15):3855-3864.
21. Mielke LA, *et al.* (2009) Tumor progression locus 2 (Map3k8) is critical for host defense against Listeria monocytogenes and IL-1 beta production. *J Immunol* 183(12):7984-7993.
22. Das S, *et al.* (2005) Tpl2/cot signals activate ERK, JNK, and NF-kappaB in a cell-type and stimulus-specific manner. *J Biol Chem* 280(25):23748-23757.
23. Tsatsanis C, *et al.* (2008) Tpl2 and ERK transduce antiproliferative T cell receptor signals and inhibit transformation of chronically stimulated T cells. *Proc Natl Acad Sci U S A* 105(8):2987-2992.
24. Kaiser F, *et al.* (2009) TPL-2 negatively regulates interferon-beta production in macrophages and myeloid dendritic cells. *J Exp Med* 206(9):1863-1871.
25. Perugorria MJ, *et al.* (2013) Tumor progression locus 2/Cot is required for activation of extracellular regulated kinase in liver injury and toll-like receptor-induced TIMP-1 gene transcription in hepatic stellate cells in mice. *Hepatology* 57(3):1238-1249.
26. Chiba N, Kakimoto K, Masuda A, & Matsuguchi T (2010) Functional roles of Cot/Tpl2 in mast cell responses to lipopolysaccharide and FcepsilonRI-clustering. *Biochem Biophys Res Commun* 402(1):1-6.
27. Serebrennikova OB, *et al.* (2012) Tpl2 ablation promotes intestinal inflammation and tumorigenesis in Apcmin mice by inhibiting IL-10 secretion and regulatory T-cell generation. *Proc Natl Acad Sci U S A* 109(18):E1082-1091.
28. Watford WT, *et al.* (2008) Tpl2 kinase regulates T cell interferon-gamma production and host resistance to Toxoplasma gondii. *J Exp Med* 205(12):2803-2812.
29. Choi HS, *et al.* (2008) Cot, a novel kinase of histone H3, induces cellular transformation through up-regulation of c-fos transcriptional activity. *Faseb J* 22(1):113-126.
30. Bandow K, *et al.* (2010) Molecular mechanisms of the inhibitory effect of lipopolysaccharide (LPS) on osteoblast differentiation. *Biochem Biophys Res Commun* 402(4):755-761.
31. Lopez-Pelaez M, Soria-Castro I, Bosca L, Fernandez M, & Alemany S (2011) Cot/tpl2 activity is required for TLR-induced activation of the Akt p70 S6k pathway in macrophages: Implications for NO synthase 2 expression. *Eur J Immunol* 41(6):1733-1741.
32. Bandow K, *et al.* (2012) LPS-induced chemokine expression in both MyD88-dependent and -independent manners is regulated by Cot/Tpl2-ERK axis in macrophages. *FEBS Lett* 586(10):1540-1546.
33. Hall JP, *et al.* (2007) Pharmacologic inhibition of tpl2 blocks inflammatory responses in primary human monocytes, synoviocytes, and blood. *J Biol Chem* 282(46):33295-33304.
34. Tsatsanis C, Patriotis C, Bear SE, & Tsichlis PN (1998) The Tpl-2 protooncoprotein activates the nuclear factor of activated T cells and induces interleukin 2 expression in T cell lines. *Proc Natl Acad Sci U S A* 95(7):3827-3832.
35. Watford WT, *et al.* (2010) Ablation of tumor progression locus 2 promotes a type 2 Th cell response in Ovalbumin-immunized mice. *J Immunol* 184(1):105-113.

36. Sugimoto K, *et al.* (2004) A serine/threonine kinase, Cot/Tpl2, modulates bacterial DNA-induced IL-12 production and Th cell differentiation. *J Clin Invest* 114(6):857-866.
37. Xiao N, *et al.* (2009) The Tpl2 mutation Sluggish impairs type I IFN production and increases susceptibility to group B streptococcal disease. *J Immunol* 183(12):7975-7983.
38. Eliopoulos AG, Dumitru CD, Wang CC, Cho J, & Tsichlis PN (2002) Induction of COX-2 by LPS in macrophages is regulated by Tpl2-dependent CREB activation signals. *Embo J* 21(18):4831-4840.
39. de Gregorio R, Iniguez MA, Fresno M, & Alemany S (2001) Cot kinase induces cyclooxygenase-2 expression in T cells through activation of the nuclear factor of activated T cells. *J Biol Chem* 276(29):27003-27009.
40. Jostins L, *et al.* (2012) Host-microbe interactions have shaped the genetic architecture of inflammatory bowel disease. *Nature* 491(7422):119-124.
41. Dunham I, *et al.* (2012) An integrated encyclopedia of DNA elements in the human genome. *Nature* 489(7414):57-74.
42. Powell DW, Pinchuk IV, Saada JI, Chen X, & Mifflin RC (2011) Mesenchymal cells of the intestinal lamina propria. *Annu Rev Physiol* 73:213-237.
43. Burczynski ME, *et al.* (2006) Molecular classification of Crohn's disease and ulcerative colitis patients using transcriptional profiles in peripheral blood mononuclear cells. *J Mol Diagn* 8(1):51-61.
44. Kabakchiev B & Silverberg MS (2013) Expression quantitative trait loci analysis identifies associations between genotype and gene expression in human intestine. *Gastroenterology* 144(7):1488-1496, 1496 e1481-1483.
45. Noble CL, *et al.* (2010) Characterization of intestinal gene expression profiles in Crohn's disease by genome-wide microarray analysis. *Inflamm Bowel Dis* 16(10):1717-1728.
46. Planell N, *et al.* (2013) Transcriptional analysis of the intestinal mucosa of patients with ulcerative colitis in remission reveals lasting epithelial cell alterations. *Gut* 62(7):967-976.
47. Nica AC, *et al.* (2011) The architecture of gene regulatory variation across multiple human tissues: the MuTHER study. *PLoS Genet* 7(2):e1002003.
48. Stranger BE, *et al.* (2012) Patterns of cis regulatory variation in diverse human populations. *PLoS Genet* 8(4):e1002639.
49. Lawrenz M, *et al.* (2012) Genetic and pharmacological targeting of TPL-2 kinase ameliorates experimental colitis: a potential target for the treatment of Crohn's disease? *Mucosal Immunol* 5(2):129-139.